"DIRECT METHANOL FUEL CELLS FOR TRANSPORTATION APPLICATIONS"

DOE/NV/11984--T1

Contract DE-AC08-96NV11984

Quarterly Technical Report

FCR-14213

November 1996

Prepared for

U. S. Department of Energy
Nevada Operations OFfice
P. O. Box 98518
Las Vegas, NV 89193-8518

International Fuel Cells

P.O. Box 739
195 Governors Highway
South Windsor, Connecticut 06074

"DIRECT METHANOL FUEL CELLS FOR TRANSPORTATION APPLICATIONS"

Contract DE-AC08-96NV11984

Quarterly Technical Report

FCR-14213

Period covered: June-Septemeber, 1996

Prepared by

T. F. Fuller
Principal Investigator
International Fuel Cells

H. R. Kunz
University of Connecticut

R. Moore
University of Southern Mississippi

Prepared for

Contracting Officer
U. S. Department of Energy
Nevada Operations Office
P. O. Box 98518
Las Vegas, NV 89193–8518

TABLE OF CONTENTS

DISCLAIMER

TABLE OF CONTENTS

FIGURE **PAGE**

SECTION I. INTRODUCTION

The purpose of this research and development effort is to advance the performance and viability of direct methanol fuel cell technology for light-duty transportation applications. For fuel cells to be an attractive alternative to conventional automotive power plants, the fuel cell stack combined with the fuel processor and ancillary systems must be competitive in terms of both performance and costs. A major advantage for the direct methanol fuel cell is that a fuel processor is not required. A direct methanol fuel cell has the potential of satisfying the demanding requirements for transportation applications, such as rapid start–up and rapid refueling. The preliminary goals of this effort are: (1) 310 W/l, (2) 445 W/kg, and (3) potential manufacturing costs of $ 48/kW.

In the twelve month period for phase I, the following critical areas will be investigated: (1) an improved proton-exchange membrane that is more impermeable to methanol, (2) improved cathode catalysts, and (3) advanced anode catalysts. In addition, these components will be combined to form membrane-electrode assemblies (MEA's) and evaluated in subscale tests. Finally a conceptual design and program plan will be developed for the construction of a 5 kW direct methanol stack in phase II of the program.

There are three principal participants in this program: (1) International Fuel Cells Corporation, (2) the University of Connecticut, and (3) the University of Southern Mississippi. The University of Southern Mississippi will develop methanol impermeable membranes, the University of Connecticut will develop methanol impermeable membranes and a redox couple. International Fuel cells will develop advanced catalysts for direct methanol fuel cells, conduct subscale testing of all membranes and catalysts, develop a conceptual design for a 5 kW stack, and manage the overall program. The program is broken into six tasks. Each is discussed in more detail below.

Task 1. Development Of Methanol Impermeable Membranes—The objective is to develop a proton exchange membrane with reduced methanol crossover and adequate electrical conductivity. Three approaches are planned, the first is the synthesis of composite membrane. Matrix-Nafion composite structures will be investigated and the characteristics of the interaction between Nafion and the composites will be determined. Porous materials, such as Teflon, polyvinylidene fluoride, polycarbonate, and alumina, that retain Nafion in a small pore matrix with pore sizes ranging from 0.03-0.6 μm will be considered. The resulting membranes shall be evaluated for methanol permeability and proton conductivity.

The second approach is synthesis of crosslinked membranes. Means to reduce the solvent (water/methanol) content of the membrane by crosslinking sulfonic acid polymers with polyamines to compress the structure of the membrane will be investigated. Amine crosslinked structures will be synthesized and evaluated for methanol permeability and proton conductivity.

The final approach is synthesis of dendrimer-modified membranes. Means to insert dendrimers into perfluorosulfonate ionomers to prevent methanol transport through the resulting membrane will be investigated. Dendrimers up to the fifth generation covering a range of sizes and functionality shall be synthesized. Solution phase processes and melt processing technology shall be employed to insert the dendrimers into the ionomers. After the dendrimers have been synthesized and processed into an ionomer film, the mechanical properties, methanol permeability, and proton conductivity of the film shall be determined.

Task 2. Advanced Catalysts For Direct Methanol Fuel Cells—The objective is to develop anode catalysts with reduced polarization for the oxidation of methanol and cathode catalyst with improved oxygen reduction activity and lower adsorption of methanol. Three activities are planned to develop advanced, higher performing anode catalysts and methanol tolerant cathode catalysts.

Advanced platinum–tantalum alloy catalysts for improved selectivity for methanol oxidation reaction rates and resistance to carbon monoxide poisoning will be investigated. The catalyst(s) will be evaluated in direct methanol fuel cells and their performance characterized as a function of the degree of alloying, stability of the alloy under fuel cell operating conditions, chemical composition, and methanol oxidation rate.

Redox couple catalysts for the oxidation of methanol or carbon monoxide will be identified. Methods of depositing and immobilizing the redox catalysts in polymer films shall be established. Electrode structures

that incorporate a co–catalyst, such as gold or platinum, shall be investigated. These electrodes shall be characterized with regard to the efficiency of the redox and co–catalyst to oxidize methanol at fuel cell operating conditions.

Cathode catalysts with improved methanol tolerance will be identified. Catalysts such as alloys of platinum/cobalt/chromium and platinum/iridium supported on carbon will be investigated. The alloy catalyst with the greatest resistance to methanol adsorption shall be formed into membrane electrode assemblies and evaluated in a DMFC.

Task 3. Direct Methanol Fuel Cell Testing—The objectives of this task are to evaluate the catalyst and membranes developed in task 1 and 2 in subscale fuel cells. The results will be used in the conceptual design of the 5 kW stack. A standard direct methanol MEA shall be tested to establish a baseline performance. Membranes developed in Task 1 showing reduced methanol permeability in out–of–cell tests shall be fabricated into MEAs for testing in fuel cell(s). These tests shall quantify methanol crossover, resistance losses, and impact on electrode performance. The best available membrane and the best catalysts from Task 2 shall be fabricated into MEAs and demonstrated in fuel cell tests.

Task 4. Performance Analysis And Conceptual Design—The objective of this task is to establish design criteria for an advanced direct methanol fuel cell stack for automotive applications. A conceptual design of the fuel cell that meets the weight and volume goals established in the solicitation shall be prepared.

Task 5. Demonstration Plan—The objective of this task is to develop a detailed plan for the Phase II construction and demonstration of the advanced direct methanol fuel cell for DOE approval. The plan shall include a description of the required tasks with a schedule and an estimate of the effort required to complete the plan.

Task 6. Management And Reporting—This task provides for management and documentation of the program. The management function performs the necessary activities to ensure that contract and technology objectives are achieved on time and within budget.

SECTION II. TECHNICAL PROGRESS SUMMARY

Task I. Development of Methanol Impermeable Membranes

Composite membrane synthesis—In this work, a variety of composite membranes are being prepared by impregnating Nafion solution into porous membranes having different pore sizes. Fine materials such as aluminum oxide, silicon carbide, and Teflon, will be mixed with Nafion solution and then will be cast as membranes. Fine powders, colloids, and porous membranes have been purchased.

A Nafion membrane of uniform 5 mil thickness was successfully fabricated in the laboratory. A commercial and an in-house prepared Nafion membranes were characterized by XRD and FTIR in addition to acid titration. The prepared membrane has similar characteristics to the commercial membrane; however, the commercial membrane is more crystalline than the membrane prepared by UCONN. A membrane methanol transport apparatus was designed, assembled, and tested. Rates of methanol transport through commercial Nafion 117 membrane were measured at room temperature. A mathematical model for methanol transport rate was developed and applied to determine the methanol diffusion coefficient. Results shows that the measured diffusion coefficient is comparable to the data in literature. Further details are provided in Appendix A.

Dendrimer-modified membrane synthesis—Initial solution–cast films of Nafion/dendrimer blends were processed using the acid–form of Nafion directly mixed with the first generation dendrimer. We have defined the percent neutralization as being moles of amine groups vs. moles of sulfonate sites. Above 70% neutralization, crosslinking between the sulfonate sites and the amine groups resulted in gelation within the blend. To bypass this gelation effect, the acid–form Nafion was neutralized with NaOH to exchange counterions to the sodium–form. The sodium–form Nafion was blended with the first generation dendrimer and then cast as a thin film. The film is then converted back into the acid–form by neutralizing it with HNO_3. Initial blend films (below 100% neutralization) showed little effect of the addition of dendrimer to preferential selectivity. However, at higher dendrimer loading (up to 500% neutralization), there is a significant decrease in the uptake of methanol. Also, the selectivity of methanol over water has been significantly reduced from values of approximately 10 to values between 1 and 2 (see the Table below and Figure 1). This behavior suggests that the dendrimers are significantly affecting the chemical nature of the ionic clusters. The resultant films are opaque with a yellow tint due to the dendrimer content, however they become transparent when hydrated. Initial attenuated total reflectance (ATR) infrared spectroscopy data has also shown that the dendrimer has remained in the membrane after the counterion exchange process.

	Methanol	**Water**
0% neutralization	163	23
100% neutralization	189	17
200% neutralization	19	16
500% neutralization	15	12

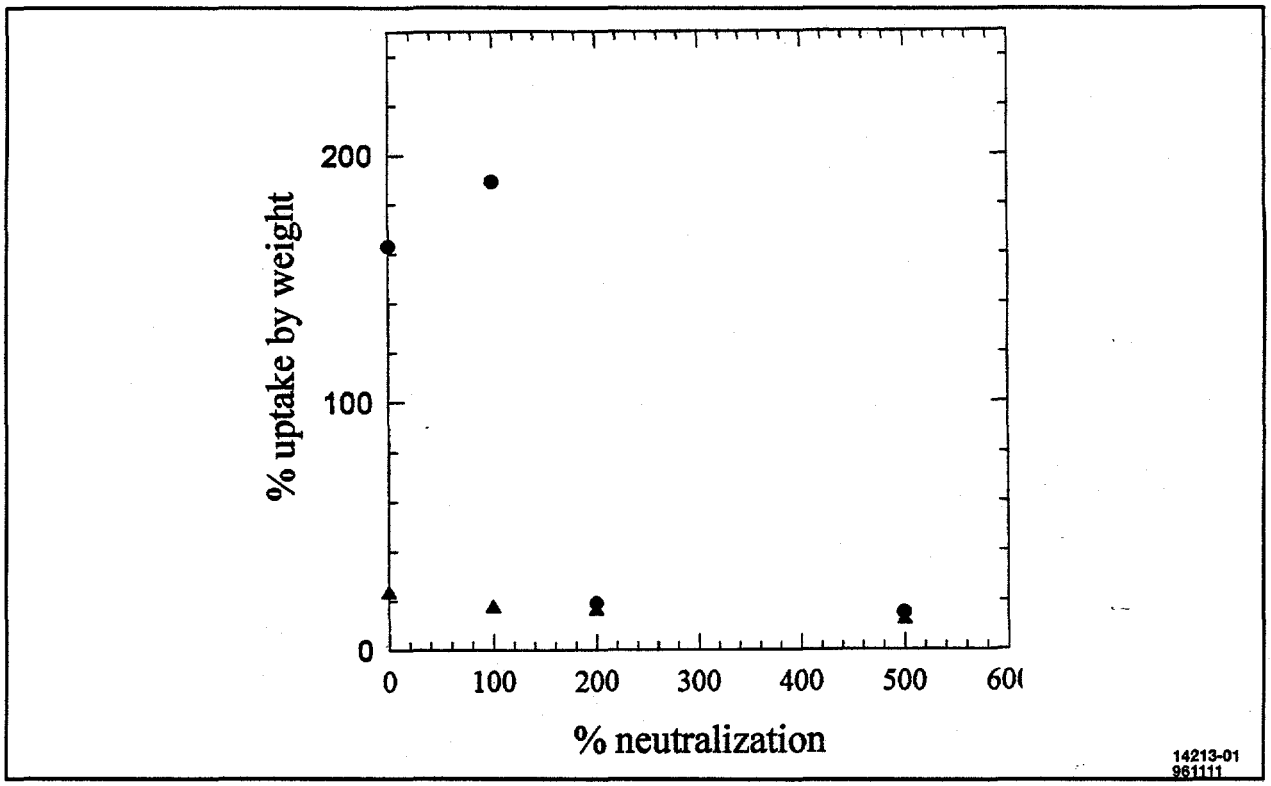

Figure 1. Solvent Uptake for Membrane as a Function of Neutralization by Dendrimer

Task II. Advanced Catalysts for Direct Methanol Fuel Cells

This task is divided into three areas: (1) advanced platinum alloy catalysts for cathodes, (2) improved binary and ternary catalysts for the anode, and (3) redox couples for the methanol anode.

Methanol tolerant cathode catalyst development—The first cathode catalyst has been prepared. This is a alloy of platinum, cobalt, and chromium. Platinum alloy catalysts were prepared using a heat treated carbon support material (Vulcan XC-72). The Brunauer, Emmet, and Teller (BET) surface area of the heat–treated material was about 90 m^2/g. The alloys were made by supporting the platinum catalyst on carbon, then impregnated these catalysts with salts (cobaltous and chromic nitrate) of the nonnoble metals. The catalysts were alloyed using a carbo-thermic reduction (i.e., nitrogen atmosphere with carbon acting as the reducing agent) process at 926°C. Chemical analysis indicate that the composition was 57.3 a/o platinum, 23.5 a/o cobalt, and 19.1 a/o chromium. The catalysts were characterized for surface area and crystal structure. The surface area was determined by hydrogen adsorption.[1] Potentiodynamic traces in 50% phosphoric acid were measured in a three-chamber rig. The working electrode was separated from a platinum counter electrode by a glass frit, and the hydrogen electrode accessed the working electrode through a Luggin capillary. The samples were cycled from -0.02 to 1.2 V relative to a reversible hydrogen electrode in the same electrolyte. The area under the reduction peaks for hydrogen adsorption was then related to exposed platinum sites assuming an average platinum density of 1.3×10^{15} atoms/cm^2 corresponding to a (100) surface of platinum with a lattice parameter of 0.392 nm. The surface area determined by this method was 44 m^2/g. The structure of the alloy is being examined with X–ray diffraction.

The catalysts were fabricated into Teflon-bonded electrodes and evaluated in a glass half-cell apparatus, described by Kunz and Gruver.[2] The electrodes contain about 30 w/o Teflon-30 and were heat-treated at 338°C. This sintering process gave the hydrophobicity level to prevent excessive flooding during testing in the half-cell apparatus. The performance of these electrodes was measured in a half–cell apparatus containing 99% phosphoric acid (Mallinkrodt) for the electrolyte. The rig was operated at 177°C and atmospheric pressure; the acid concentration was maintained at 99% by saturating the gas reactants with water to a dew point of 60°C.

The activity of this catalyst was 30 mA/mg Pt. This is the current density at 0.9V on oxygen relative to a hydrogen electrode. The performance at 200 ASF (215 mA/cm^2) was 720 mV. This cannot be related directly to the performance in PEM/DM fuel cells, but can be used as a relative measure of the ability of the catalyst to reduce oxygen.

A second cathode catalyst is being prepared. This is an alloy of platinum and iridium.

Anode catalyst development—Three anode catalysts have been prepared. These are all unsupported metal blacks prepared by the Adams method.[3] Pt/Ru, Pt/Ta, and Pt/Ru/Ir anode catalysts have been prepared. The chemical analyses and BET surface areas are summarized in the table below. XRD analysis is in progress.

Catalyst	Composition	BET surface area
Pt/Ru	$Pt_{0.52}$ $Ru_{.0.48}$	72.6 m^2/g
Pt/Ru/Ir	$Pt_{.0.52}$ Ru.25 $Ir_{0.24}$	58.4
Pt/Ta		30.2

The platinum ruthenium is the baseline material. The performance of this material is discussed in the next section on direct methanol fuel cell testing.

1 S. Gilman, *J. Phys. Chem.*, **67**, 78 (1963).

2 H. R. Kunz and G. A. Gruver, *J. Electrochem. Soc.*, **122**, 1279 (1975).

3 K. Kinoshita and P. Stonehart, "Preparation and Characterization of Highly Dispersed Electocatalytic Materials," *Modern Aspects of Electrochemistry*, J. O'M. Bockris and B. E. Conway, ed., Plenum Press, New York (1977).

Redox couple catalysts—Through a review of the literature, a methodology was developed for the selection of metal macrocycles as co–catalysts with platinum for the direct electrochemical oxidation of methanol. These catalysts consist of phthalocyanines, porphyrins, and tetraaza–macrocyclic complexes with various central metals. Commercially available catalysts are being purchased and others are being prepared at UCONN. An experimental rig was constructed for the voltammetric characterization of these catalysts and their performance evaluation as methanol catalysts. Preliminary experiments show that the experimental facility is capable of providing the needed data. Details of the work at UCONN are provided in appendix A.

Task III. Direct Methanol Fuel Cell Testing

The first step is to standardize all of the tests and to establish the baseline performance. Membrane electrode assemblies were fabricated from platinum black cathodes, Nafion 117 membrane, and platinum ruthenium anodes. Performance established on other IFC programs has been duplicated with these materials. This represents the baseline performance.

Methanol Test Plan

Cell operating conditions—The cells are evaluated under the following conditions:

- 80°C
- ambient pressure
- dry O_2 or air on cathode
- low utilization of reactants (1000 cc/min for hydrogen or oxygen, 3000 cc/min for air, and 3 cc/min methanol).
- 1 molar methanol on the anode

Test protocol

After the cells are started up, the following tests will be performed on all cells:

1. methanol oxygen polarization
2. methanol air performance
3. crossover on air
4. anode polarization

As part of these tests, the cell iR will be measured by current interruption. The crossover is determined by measuring the carbon dioxide content in the cathode exhaust. The anode polarization is measured by evolving hydrogen on the cathode and oxidizing methanol on the anode. Since the kinetics for the hydrogen electrode are facile, this is a good measure of the anode polarization. The key parameter from these measurements are summarized in the table below.

Cell designation	iR at 100 mA/cm^2 (mV)	Anode activity mA/mg Pt at 0.2 V	Cell potential on air at 215 mA/cm^2 (V)	Equivalent CH_3OH crossover at 11 mA/cm^2 on air (mA/cm^2)
Baseline	20	1	0.34	185

Baseline performance—Two performance curves are included in Figures 2 and 3. The first is the anode polarization. This represents the activity of the anode catalyst in oxidizing methanol. As can be seen on the semi-log plot in Figure 2, at low current densities, the curve is linear. This portion of the curve is the best representation of the catalytic activity of the catalyst. At higher current densities, the polarization increases rapidly, this is a combination of the catalytic activity and the structure of the electrode, i.e., ohmic and mass-transfer limitations.

Figure 3 shows the performance of the full cell. Operating conditions are ambient pressure, 80°C, with the cell on air and 1 molar methanol.

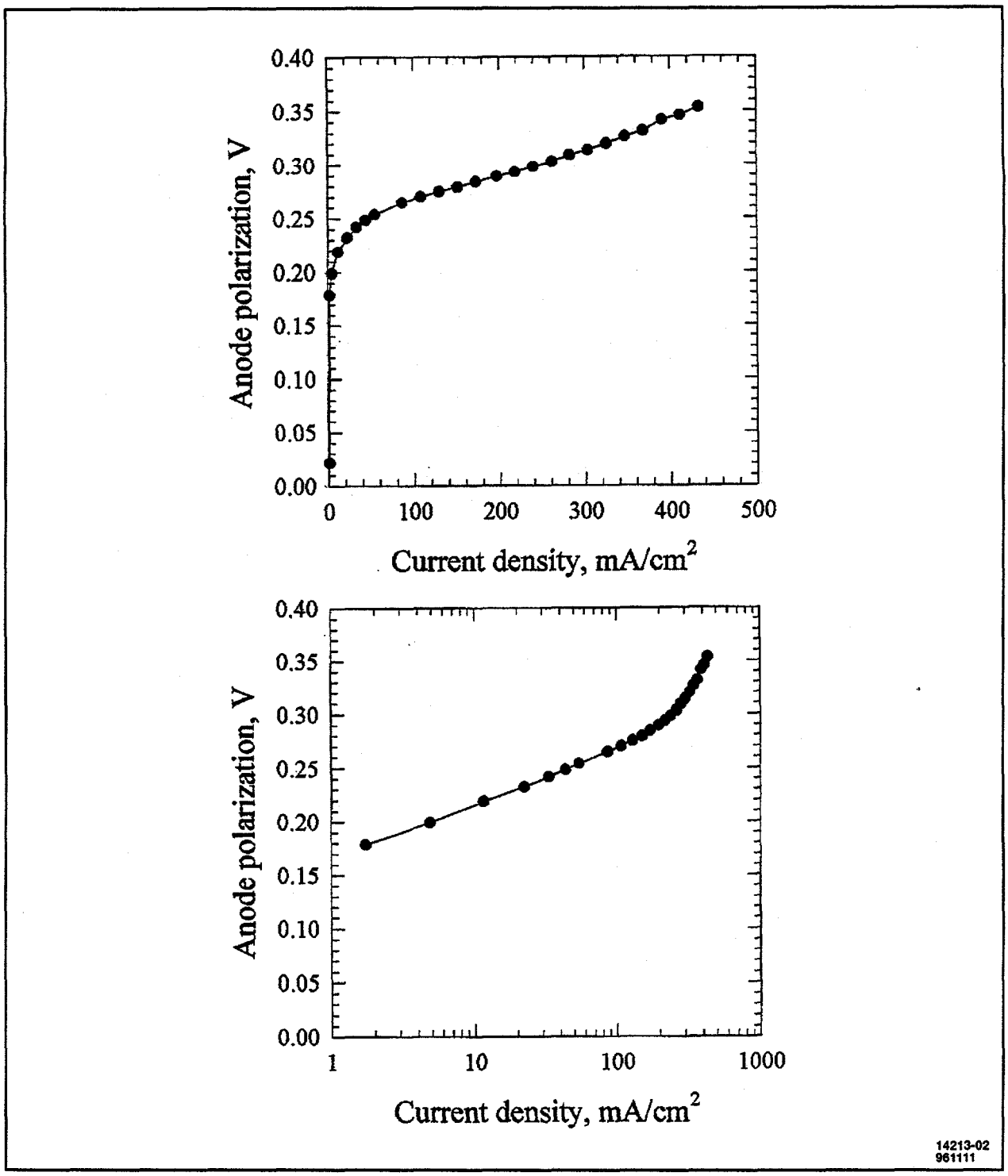

Figure 2. Anode Performance Polarization of Standard Platinum Ruthenium Black. Temperature of Cell is 80°C.

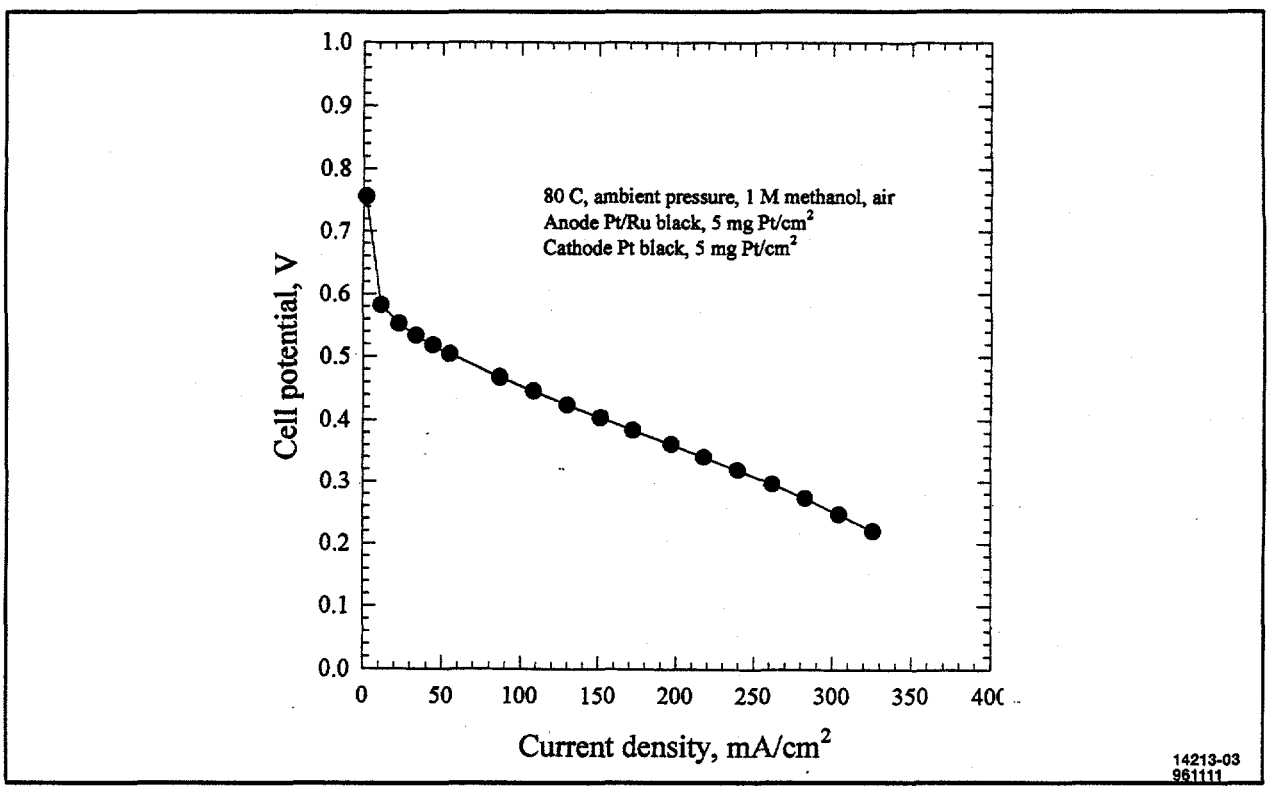

Figure 3. Methanol Air Performance of Baseline Materials

Task IV. Performance Analysis and Conceptual Design

The conceptual design will be for a power plant that would deliver 50 kW of net power to the vehicle at about 250 V. The following design criteria are established as a first step in developing the conceptual design. The objective is to meet the weight and volume goals and simultaneously make the power plant as transparent to the user as possible.

Weight and volume—The goals established in the solicitation are 445 W/kg and 310 W/l for the power plant. This results in a total system weight of 112 kg and a total volume of 161 liters. These goals are extremely challenging compared to the present state of the art direct methanol cells. For example, we are developing a 300 W direct methanol fuel cell power module under a DARPA contract. This has a specific power of about 55 W/kg. This includes the weight of the fuel and because of the small size, the ancillary components make up a larger fraction of the system weight than they will for a larger power plant. Good individual cell performance has been reported by a number of research groups. Typically, these were at elevated temperatures and pressure and with very high flow rates. The system performance will be the target and not the individual cell performance.

Transient throttle response—The objective is to achieve a full power transient in 200 ms. The ambient pressure direct methanol system has two advantages in this respect. First, operation at ambient pressure eliminates the throttle response lag that may exist in pressurized systems. Second, because reforming of the fuel is not required, the response of the fuel processor, a critical problem for methanol reforming, is eliminated. The response of the membrane electrode assembly is very fast. Any additional problems can be corrected with feed forward control.

Normal start time—The goal is for the power plant to supply rated power within five seconds of the supply of reactants to the stack at ambient pressure.

Cold weather start—The goal is to permit shutdown, storage at –40°C, and start up from this temperature. All PEM power plants require management of humidification water at freezing conditions.

Hot weather limitation—The goal is to allow operation at ambient temperatures up to 50°C.

High rate manufacturing cost.—For the initial design it is assumed that the catalyst loading of 1.0 mg Pt/cm^2 for the cathode and 5 mg Pt/cm^2 for the anode. It is recognized that this is not consistent with the ultimate cost goals of $48 /kW.

Water and thermal balance—The fuel-cell system must be designed to be in water and thermal balance. The only practical method of cooling a mobile, nonmarine power plant (not necessarily the cell stack) is air cooling. Since ambient pressure operation is anticipated, the utilization of air is not critical and is not a specific criterion. However, the utilization of air will have a major impact on the thermal and water management.

Emission—No emission of methanol from the power plant. 100 percent fuel efficiency is desired. Any fuel not consumed at the anode will have to be oxidized to prevent methanol emissions.

Automatic controls—A control system is required to maintain thermal and water balance under steady-state and transient conditions.

Task 5. Demonstration Plan

No work was scheduled or accomplished on this task during the period covered by the report.

SECTION III. CURRENT PROBLEMS

Task I. Development of Methanol Impermeable Membranes

Composite membrane synthesis—Composite membranes using Teflon as the filler material was originally planned to be obtained from W. L. Gore & Associates, Inc. since such membranes had previously been supplied to another researcher.[4] However, W. L. Gore views UCONN as a competitor; and as a result, these materials are not available for use by UCONN. W. L. Gore is willing to provide membranes to IFC, but would like to limit the disclosure of the results of our evaluation. This task is also behind schedule because of the late start of the subcontract and student availability.

Dendrimer—The solvent uptake data for the pure Nafion and the blend containing 100% neutralization are abnormally high. We suspect that the critical casting temperature was too low, which resulted in a low level of polymer crystallinity. Since the crystalline domains act as barriers to solvent swelling, the low casting temperatures produced a morphology, which allowed for the unusually high uptake.

Crosslinked amine—No work has yet been started on this task because of the late start of the subcontract with UCONN and the time necessary to obtain a person at the University of Iowa to assist in this task. Because of this lost time, a post–doctoral employee is being recruited and should become available early in the next quarter. The use of a post–doctoral employee rather than a graduate student should help to accelerate this task.

Task II. Advanced Catalysts for Direct Methanol Fuel Cells

Redox couple catalysts—Initial experiments with NiPC and CoPC have established the methods by which monolayers of the macrocycles can be deposited on carbon. However, coverages calculated from the charge under the peaks in cyclic voltammograms were less than calculated from the adsorption procedure. One explanation may be that the electrodes were incompletely wetted by electrolyte during voltammetry. If this proves to be the case then procedures for assuring complete utilization of the catalysts in practical electrodes will have to be developed.

Because the subcontract between UCONN and International Fuel Cells started one month after the contract between IFC and DOE, the work being performed at UCONN is behind schedule. An additional problem resulted because the subcontract started during the summer when students already had other scheduled activities. Some of this lost time will be recovered through the use of more post–doctoral participants rather than graduate students.

Task III. Direct Methanol Fuel Cell Testing

Making the transition from high loaded platinum black cathode catalysts to low loaded supported catalysts will require some optimization of the electrode structure. Although we have experience in making low loaded supported electrodes for PEM fuel cells, these have not been made for direct methanol cells previously. Achieving an acceptable structure will require more testing than originally anticipated. This may delay the selection of the cathode catalyst, but will not affect the overall program schedule.

4 E.J. Taylor, C. Pazienza, R. Waterhouse, and G. Wilemski, "The Effect of Support Morphology on Composite Membrane Performance", The Electrochemical Society, Proceedings Vol. 86–2, Abstract No. 590, pp. 883 (1986).

SECTION IV. WORK PLANNED

Task I. Development of Methanol Impermeable Membranes

Composite membrane synthesis—During the next quarter, Nafion solution will be impregnated into polyvinylidene fluoride (PVF) membranes with various pore sizes in order to investigate the effect of pore sizes on the methanol transport. Fine powders such as silicon carbide and aluminum oxide as well as Teflon colloids will be mixed with Nafion solutions and then will be cast as composite membranes. Composite membranes will be characterized by various techniques and tested for the methanol transport. Ionic conductivity of the various membranes will be determine using AC impedance spectroscopy.

Dendrimer—Higher generations of dendrimer will be synthesized and examined by NMR for purity. Blends of the higher generation dendrimers and Nafion will be solution–cast and characterized by FTIR, DMA, and solvent uptake studies. Small angle X–ray scattering (SAXS) will be performed on the blended film samples to determine what effect the variable percent neutralizations and dendrimer generations have on the morphology of the membrane. AC impedence studies will be conducted on these membranes in order to evaluate the effect of dendrimer incorporation on the proton conductivity.

Crosslinked amines—Synthesis of Nafion membranes that have crosslinking will begin. These membranes will be characterized with respect to conductivity, water transport, and methanol transport.

Task II. Advanced Catalysts for Direct Methanol Fuel Cells

Methanol tolerant cathode catalyst development—The second alloy catalyst will be completed. XRD, electrochemical area, and half-cell evaluation will be completed. If time allows, a third alloy catalyst will be prepared.

Anode catalyst development—The catalyst already prepared will be evaluated in full cells. XRD analysis of these materials will also be completed.

Redox couple—During the next quarter voltammograms will identify the electrochemical redox behavior of the various macrocycles. They will be screened for their activity for the catalysis of methanol oxidation, with and without platinum co–catalyst. The relationship between the redox behavior and catalyst activity will be examined to identify a catalyst system for optimization. Metal complexes of tetramethyl–tetraazacyclotetradecane will be synthesized at the University of Connecticut and will be included in the catalyst screening program as they become available.

Task III. Direct Methanol Fuel Cell Testing

Development of the cathode catalyst will continue. The anode and cathode catalysts prepared will be evaluated in full cell tests. At the end of the next quarter/ beginning of the third quarter, initial membrane samples are anticipated.

Task IV. Performance Analysis and Conceptual Design

Conceptual design of the fuel cell power plant for automotive application will continue.

Task V. Demonstration Plan

No work is planned for the next quarter on this task.

SECTION V. SCHEDULE STATUS

Schedule and Milestones Chart

ID	Task Name
1	**Task 1.CH3OH Imp. Membrane**
2	Retain Nafion in matrix
3	Crosslinked membrane
4	intial UCONN samples
5	Dendrimer modified membrane
6	initial S. Miss. sample
7	low crossover membrane established
8	**Task 2. Advanced Catalyst**
9	**Cathode catalysts**
10	Pt-Co-Cr & Pt-Ir-Cr catalysts
11	catalyst characterization
12	cathode catalyst est
13	Redox couple
14	initial redox samples
15	**Anode catalysts**
16	Pt/Ru catalyst
17	Pt-Ta &Pt-Ir-Ru catalyst
18	catalyst characterization
19	half cell evaluation
20	anode catalyst est.
21	**Task 3. DMFC Testing**
22	test stand preps
23	establish baseline
24	anode MEA
25	cathode MEA
26	U. S. Miss. membrane
27	UCONN membrane
28	redox couple
29	single cell demonstrated
30	**Task 4. Perf. Anal. & Design**
31	design criteria

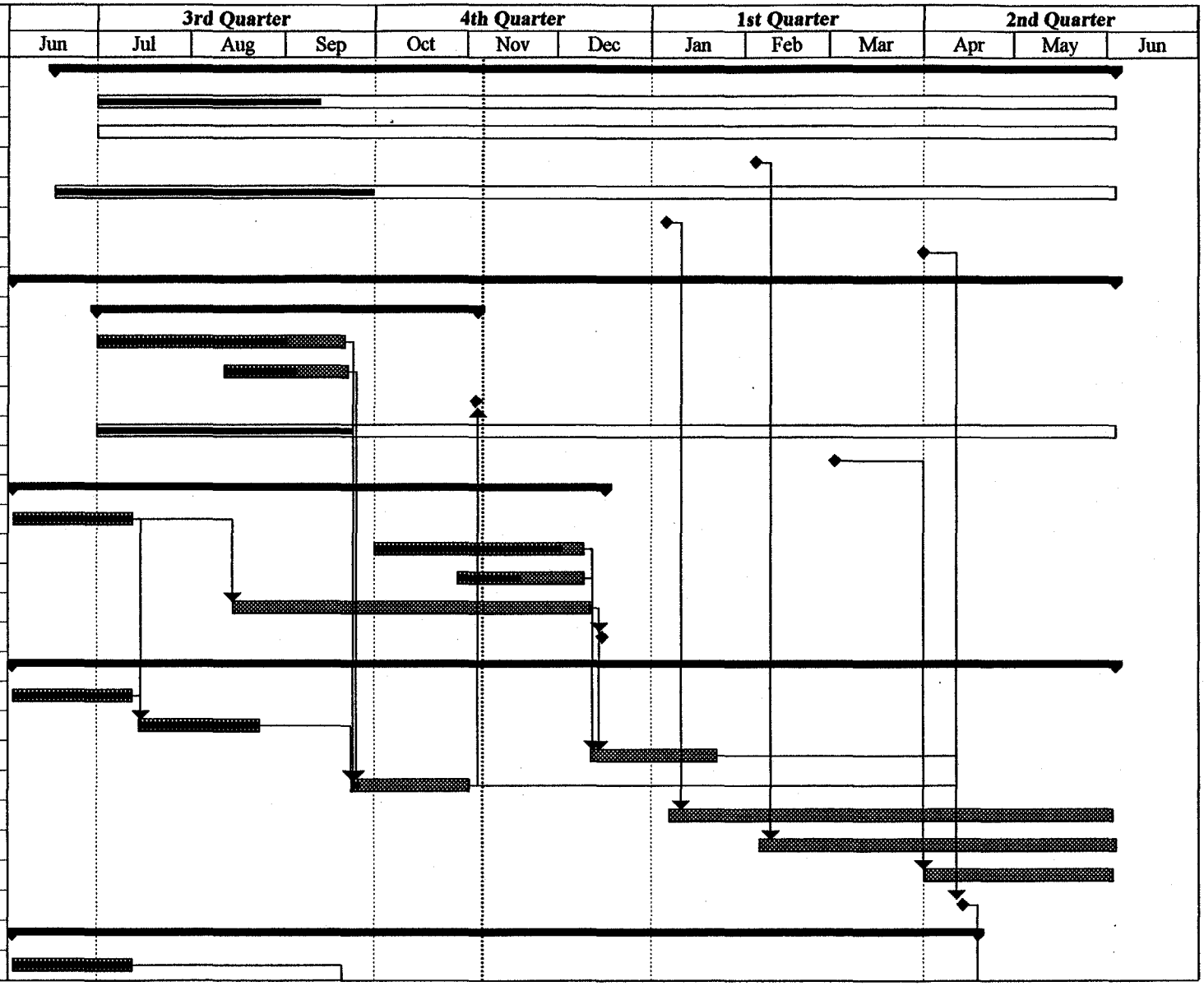

Project: DOE DMO Program
September 30, 1996

Task
Progress
Milestone
Summary
Rolled Up Task
Rolled Up Milestone ◇
Rolled Up Progress

Schedule and Milestones Chart

ID	Task Name	3rd Quarter			4th Quarter			1st Quarter			2nd Quarter		
		Jun	Jul	Aug	Sep	Oct	Nov	Dec	Jan	Feb	Mar	Apr	May	Jun
32	conceptual design													
33	design concept completed													
34	**Task 5. Demonstration Plan**													
35	Phase II plan													
36	Phase II plan accepted													
37	**Task 6. Management and Reporting**													
38	monthly and quarterly													
39	Final report													

Project: DOE DMO Program
September 30, 1996

Task
Progress
Milestone
Summary
Rolled Up Task
Rolled Up Milestone ◇
Rolled Up Progress

SECTION VI. COST PERFORMANCE REPORT

FCR-14160

DOE F1332.12
(11-84)

U.S. DEPARTMENT OF ENERGY

COST PERFORMANCE REPORT – WORK BREAKDOWN STRUCTURE (Format 1)

Page of
FORM APPROVED
OMB NO. 1901–1400

1. TITLE	2. REPORTING PERIOD	3. IDENTIFICATION NUMBER
ADVANCED FUEL CELLS FOR TRANSPORTATION APPLICATIONS	September 1996	DE-AC08-96NV11984
4. PARTICIPANT NAME AND ADDRESS: International Fuel Cells Corporation, 195 Governor's Highway, P. O. Box 739, South Windsor, CT 06074	5. COST PLAN DATE: 7/5/96	6. START DATE: May 28, 1996
		7. COMPLETION DATE: June 30, 1997

4. NEGOTIATED COST	9. ESTIMATED COST OF AUTHORIZED UNPRICED WORK	10. TARGET PROFIT/FEE %	11. TARGET PRICE	12. ESTIMATED PRICE	13. SHARE RATIO	14. CONTRACT CEILING	15. ESTIMATED CEILING
$729,283	0	0	$729,283	$729,283	71/29	$729,283	$729,283

16. WBS ELEMENT	CURRENT PERIOD					CUMULATIVE TO DATE					AT COMPLETION		
	BUDGETED COST		Actual Cost of Work Performed	VARIANCE		BUDGETED COST		Actual Cost of Work Performed	VARIANCE				
	Work Scheduled	Work Performed		Schedule	Cost	Work Scheduled	Work Performed		Schedule	Cost	Budgeted	Revised Estimate	Variance
TASK 1	19	19	16	0	3	37	37	16	0	21	222		
TASK 2	18	18	24	0	(6)	45	45	39	0	6	197		
TASK 3	4	4	4	0	0	15	15	13	0	2	61		
TASK 4	4	4	1	0	3	12	12	5	0	7	30		
TASK 5	0	0	0	0	0	0	0	0	0	0	39		
TASK 6	4	4	1	0	3	19	19	12	0	7	62		
17. WBS SUBTOTAL	49	49	46	0	3	128	128	85	0	43	611	611	
18. COST OF MONEY	–	–	–	–		–	–	–	–		–	–	
19. GENERAL & ADMIN.	9	9	5	0	4	24	24	10	0	14	118	118	
20. UNDISTRIBUTED BUDGET													
21. SUBTOTAL	58	58	51	0	7	152	152	95	0	57	729	729	
22. SHARE	25	25	30	0	(5)	74	74	111	0	(37)	296	296	
23. TOTAL	83	83	81	0	2	226	226	206	0	20	1.025	1.025	0
	RECONCILIATION TO CONTRACT BUDGET BASE												
24. VARIANCE ADJUSTMENT													
25. TOTAL CONTRACT VARIANCE													

26. DOLLARS EXPRESSED IN:	27. SIGNATURE OF PARTICIPANT'S PROJECT MANAGER	28. DATE
THOUSANDS	J Fuller	10/25/96

SECTION VII. VARIANCE ANALYSIS

The cost variance for Tasks 1 and 2 shown in the cost performance report is the result of slow invoicing by the universities. Both the University of Southern Mississippi and the University of Connecticut have just recently started sending invoices on a monthly basis. Since the work is nearly on schedule, this is represented as a cost variance rather than a schedule variance, and the cost of the program appears low.

APPENDIX A. UCONN REPORT

Direct Methanol Fuel Cell for Transportation Applications

First Quarterly Report to International Fuel Cells
under Contract No. DE-AC08-96NV11984

October 15, 1996

Principal Investigators:
James M. Fenton
H. Russell Kunz

University of Connecticut
Department of Chemical Engineering
Environmental Research Institute
191 Auditorium Road, Box U-222
Storrs, CT 06269-3222

Contributors to this report consist of:

University of Connecticut

Department of Chemical Engineering
Anthony J. Aldykiewicz
John A.S. Bett
Michael B. Cutlip
James M. Fenton
Chunzhi He
H. Russell Kunz
Jung-Chou Lin
William Ray

Department of Chemistry
William F. Bailey
Dominic V. McGrath

University of Iowa

Department of Chemistry
Johna Leddy

Direct Methanol Fuel Cell for Transportation Applications

Abstract

This report describes the work performed at the University of Connecticut during the first quarter under a subcontract with International Fuel Cells on Contract DE-AC08-96NV11984 with the U.S. Department of Energy. Research is being performed on two topics that are critical to the commercialization of direct methanol fuel cells for vehicular use. These topics are an active anode catalyst for the direct oxidation of methanol and a proton exchange membrane that reduces the migration of methanol from the cell anode to the cathode. In this period, experimental facilities were constructed for the performance of the tasks and preliminary experiments begun.

I. Introduction

Proton exchange membrane (PEM) fuel cells offer the potential for an efficient and clean replacement for the internal combustion engine in vehicular applications. In order to gain a significant segment of the market, the fuel that is used must meet safety, storage, availability, cost, and environmental requirements as well as have the potential that a suitable infrastructure could be formed. Of the candidate fuels, methanol appears to be the most desirable.

Since the vehicular application of fuel cells requires a compact power plant with fast time response, the direct electrochemical oxidation of methanol at the fuel cell anode is highly desirable. However, the rate of direct oxidation of methanol in the cell is slow even with the best available catalysts. A fuel processor to convert the methanol to hydrogen for a faster anode reaction would involve additional components operating at higher temperatures than the fuel cell and add to system volume, weight, response time, and cost. Therefore, a new anode catalyst is needed for the direct electrochemical oxidation of methanol.

Methanol also presents another problem because of its high solubility in the PEM. Methanol on the fuel side of the cell can migrate through the membrane to the cathode side where it is chemically oxidized by the air, resulting in a loss of cell efficiency and a reduced cathode performance. Therefore, a membrane with a reduced methanol transport rate is needed. Although a cathode catalyst might be developed that does not oxidize this methanol, the methanol would still migrate through the cell and be present in the air effluent. Removal of this methanol would be needed to restore the lost efficiency and eliminate air pollution from the methanol.

Because of the needs for a new catalyst for the direct oxidation of methanol and new membranes with reduced methanol flux, a program was started at the University of Connecticut (UCONN) under a subcontract with International Fuel Cells (IFC) in U.S. Department of Energy Contract No. DE-AC08-96NV11894, Direct Methanol Fuel Cell for Transportation Applications.

The specific work statement of the UCONN subcontract is as follows:

Task 1.0: Direct Methanol Catalyst

The Seller shall identify redox couple catalysts for the oxidation of methanol or carbon monoxide. Methods of depositing and immobilizing the redox catalysts in polymer films shall be established. Electrode structures that incorporate a co-catalyst, such as gold or platinum, shall be investigated. These electrodes shall be characterized with regard to the efficiency of the redox and co-catalyst to oxidize methanol at fuel cell operating conditions. A sample of the best catalyst will be submitted to Buyer for evaluation.

Task 2.0: Physically Modified Proton Exchange Membrane

The Seller shall investigate matrix Nafion composite structures and determine the characteristics of the interaction between Nafion and the composites. Porous materials, such as Teflon, polyvinylidene fluoride, polycarbonate, and alumina, that retain Nafion in a small pore matrix with pore sizes ranging from 0.03 - 0.6 μm shall be considered. The resulting membranes shall be evaluated for methanol permeability and proton conductivity. Samples of the best membrane will be provided to Buyer for evaluation.

Task 3.0: Chemically Modified Proton Exchange Membrane

The Seller shall investigate means to reduce the solvent (water/methanol) content of the membrane by crosslinking sulfonic acid polymers with polyamines to compress the structure of the membrane. The Contractor shall synthesize amine crosslinked structures and evaluate them for methanol permeability and proton conductivity. Samples of the best membrane will be provided to Buyer for evaluation.

Task 4.0: Reporting

The Seller shall prepare and submit to Buyer a Final Technical Report on Phase I activities, describing all significant work performed during the entire period of the Subcontract.

The Seller shall prepare and submit to the Buyer a Technical Progress Report quarterly based upon the U.S. Government's fiscal year. This report is due on the fifteenth day of the month following the close of the applicable quarter. This report shall communicate an assessment of Subcontract status, explain variances and problems, report accomplishments, and discuss any other areas of concern or achievement.

The Seller shall submit to Buyer via electronic mail or facsimile, a brief (no more than one page) biweekly report describing significant program actions or events.

This report presents the results of the work performed at UCONN on this contract for the period from July 1 to September 30, 1996 and fulfills the requirements of the first quarterly report as described in Task 4 above.

II. Technical Progress

A. Task 1.0: Direct Methanol Catalyst

1. Summary

Through a review of the literature a methodology was developed for the selection of metal macrocycles as co-catalysts with platinum for the direct electrochemical oxidation of methanol. These catalysts consist of phthalocyanines, porphyrins, and tetraaza-macrocyclic complexes with various central metals. Commercially available catalysts are being purchased and others are being prepared at UCONN. An experimental rig was constructed for the voltammetric characterization

of these catalysts and their performance evaluation as methanol catalysts. Preliminary experiments show that the experimental facility is capable of providing the needed data.

2. Selection of Metal Macrocycles for Evaluation as Catalysts (J.A.S. Bett)

Few reports in which metal macrocycles have been evaluated as catalysts for methanol electro-oxidation are available in the literature. In a preliminary survey for this program only two references were identified: Sarangapani (1) claimed that platinum, with an unspecified macrocycle as a co-catalyst, was active for methanol oxidation, while Lai and Wong showed that a ruthenium bipyridylethylenediamine was active, but at very high overvoltage(2).

For oxygen electro-reduction, in contrast, macrocycle complexes such as the phthalocyanines and porphyrins have been evaluated as catalysts for many years and an extensive literature has accumulated. Cobalt and iron phthalocyanines and porphyrins have shown some activity although rates, lower than for platinum, were not sufficient to be practical for fuel cells with acid electrolyte (3)(4). Because they had low electronic conductivity in bulk crystalline form the macrocycles were dispersed on high surface area carbon supports for inclusion in practical electrodes. In some cases the most active catalysts resulted when the carbon-supported catalysts were pyrolyzed at temperatures up to 900°C (5). After this treatment the active state of the catalyst was shown to contain free metal as a phase oxide. However, in some cases it was

claimed that the metal ion in its ring of nitrogen ligands was fused to the carbon surface by the pyrolysis.

Attempts to understand the mechanism by which the macrocycles accelerated oxygen reduction have emphasized the role of the central cation. For some macrocycles the proposed mechanism required the central ion to adsorb oxygen and transition through two oxidation states during the charge transfer process , e.g. Zagal et al.(6) For these, the redox potential of the cation must lie in the potential range where catalysis occurred. For other macrocycles, oxygen reduction occurred well below the redox potential for the cation so that catalysis did not appear to operate via such a redox mechanism, e.g. Durand and Anson (7).

Platinum/ruthenium metal alloy has been shown to be the most active catalyst for methanol oxidation. Studies of this surface have suggested that the reaction occurs by dissociative adsorption of methanol on platinum sites to form a strongly adsorbed reaction intermediate that may be carbon monoxide. In parallel, at higher levels of polarization, water adsorbs and dissociates on ruthenium sites to provide a hydroxylic species that subsequently oxidizes the carbon monoxide. The dissociation of water occurs on ruthenium at lower potentials than on platinum, resulting in enhanced activity for platinum-ruthenium over pure platinum (8).

Clearly, the central ion in macrocyclics can promote the oxidative dissociation of water. For example, the pH dependence of the $Co^{2+/3+}$ redox couple in Co porphyrin adsorbed on carbon (above pH 6) suggests the reaction (7):

$$[LCo^{III}OH]^{+2} + H^{+} + e \quad <-> \quad [LCo^{II}OH_2]^{+2}$$

In contrast, there is no precedent for dissociative reaction of methanol on macrocycles and for this reason we propose to evaluate the ability of platinum to act as co-catalyst by analogy with the dual site nature of platinum/ruthenium catalysts. Thus, oxidizing species generated from water by the metal macrocycle will be supplied to the platinum surface to react with adsorbed methanol. The intent will be to evaluate a range of macrocyclic complexes to identify candidates that may dissociate water to provide oxidizing species at potentials below the 0.3V limit set presently by the properties of ruthenium in platinum-ruthenium alloy.

Therefore, as a guide to selection of candidates for evaluation, the literature was reviewed for information regarding the effect of

complex formation and adsorption or attachment to a carbon support on the redox potential of the central ion.

In a series of papers Kadish (9,10 11) and his co-workers have determined the redox potentials of iron porphyrins with various substituent groups attached to the nitrogen ligands surrounding the iron. In non-aqueous electrolyte they showed that electron withdrawing substituents shift the potential anodically and electron donating groups shift potential cathodically relative to the redox potential of the unsubstituted porphyrin. Over a range of substituents from strongly electron withdrawing ($p\text{-}NO_2$) to strongly electron donating ($p\text{-}OCH_2Ph$) the redox potential was changed by up to +/- 150 mv from the initial value. The qualitative direction for these effects is readily understood; electron withdrawing substituents reduce the extent of electron donation from the nitrogen ligands to the metal cation thereby making more stable the higher oxidation state of the metal.

Even larger effects were observed when the axial ligands, above and below the plane of the complex, were varied. Almost two (2.0) volts difference in potential was observed between fluoride and nitroso axial ligands.

Table 1 lists redox potentials for cobalt, iron and ruthenium complexes reported in papers where they had been evaluated as catalysts for oxygen reduction. Except where otherwise noted the electrolyte was a strong aqueous acid, generally sulfuric.

For the cobalt complexes the redox potential of $Co^{2+/3+}$ was lowered from 1.808 volts for the free ion in acid solution to about 1.0 volt for the phthalocyanine and 0.76 volts for the tetraphenylporphyrin (12). The phthalocyanine complexes, whether in solution or adsorbed on carbon for use as heterogenous catalysts, had about the same redox potential (13,14). Thus adsorption on carbon did not change the potential significantly from that of the dissolved complex. This behavior was reported in a number of studies and even pyrolysis of the adsorbed complex at high temperature, in case of iron phthalocyanine, did not appear to change the potential of the original complex.(15). This would support the conclusion that the iron with its surrounding nitrogen ligands, survived mild pyrolysis intact on the carbon surface.

Table 1 shows that the porphyrin complex lowered the redox potential for cobalt by an even greater amount than the phthalocyanine. The same sequence was also demonstrated for the

iron complexes; again the porphyrin complexes had lower potentials than the phthalocyanines. Apparently, the extent of electron donation by the nitrogen ligands was less in the phthalocyanines than in the porphyrins due to the presence of the electron withdrawing, fuzed aromatic rings in the phthalocyanines.

The series of m aminophenylporphyrins studied by Kobyashi et al. (16) clearly demonstrated that the redox potential was raised by electron withdrawing substituents, as Kadish noted for porphyrins in solution.

Only one of the ruthenium complexes listed in Table 1 is a porphyrin, but these also show that nitrogen ligands tend to lower the formal redox potential of the central ion.

A strategy for the search for a catalyst for methanol oxidation was formulated using the brief review described above. Table 1 showed that major changes in the redox potential of the central ion were affected by change of the ligand from phthalocyanine to porphyrin. This was due to the difference in extent of electron donation, or basicity, of the nitrogen ligands in the two macrocycles. Therefore, in this program the activity of a number of macrocyclic complexes that provide a range of basicity of the nitrogen ligands will be evaluated. These will include phthalocyanine, porphyrin and in addition tetraaza-macrocyclic complexes.

The phthalocyanine and porphyrins have been discussed above. The tetraaza-macrocycles offer an extension of the range of basicity of the nitrogen ligand. In these compounds the chelating ring surrounding the metal ion is comprised of saturated bonds and the nitrogen ligands are in a tertiary, sp_3 bonding state that is more strongly electron donating than the unsaturated, sp_2 state of the phthalocyanine and porphyrins. They are known to stabilize transition metal ions in unusual (high) oxidation states.(17,18,19) The expected order of basicity, or stabilization of the higher oxidation states of the metal ion, or lowering of the oxidation potential, will be:

phthalocyanine < porphyrin < tetraaza-macrocycle

For each ligand type a number of central metal cations will be evaluated. This will offer a range of properties of the ion, such as d-orbital occupation, and of ligand strength. It was reasoned that if a promising candidate were identified, its redox potential

could be "fine tuned" by the addition of appropriate substituents to the ligand, as described by Kadish.

3. Catalyst Preparation and Evaluation (J.A.S. Bett, W.F. Bailey, D.V. McGrath, A.J. Aldykiewicz)

The specific macrocycles that have been selected for evaluation are listed in Table 2. The phthalocyanines and tetramethoxyphenyl porphyrins are available commercially. The tetramethyl-tetraazacyclotetradecane will be synthesized at the University of Connecticut.

The phthalocyanines and tetramethoxyphenyl porphyrins were selected in part because the conditions for adsorption of these complexes as monolayers on carbon have already been established in studies of their activity for oxygen reduction (3,4). As discussed above, the macrocycles were dispersed on high surface area carbon supports for inclusion in practical electrodes because of their low conductivity. Phthalocyanines and tetramethoxyphenyl porphyrins were shown to adsorb on carbon black from pyridine and acetone solution with Langmuirian isotherms that indicated the formation of well defined monolayers of the adsorbed complexes.

The surface population of the complexes at the monolayer level tended to be low, with about 600 to 800 nm^2 per molecule, suggesting planar adsorption. The redox behavior of the adsorbed complexes indicated good electronic contact with the carbon surface.

For their initial evaluation in this program, the macrocycles were adsorbed in similar manner on Vulcan XC-72 carbon black. Subsequently, platinum crystallites will be dispersed on the monolayer of macrocycle to investigate the possibility for co-catalysis. Alternatively, the macrocycle will be adsorbed on a carbon black previously catalyzed with platinum.

The catalyzed powders have been prepared as electrodes on carbon paper. The catalyst layer, containing 5% by weight of Teflon, was precipitated or applied as a paste to the paper so that, after sintering, the loading was approximately 1 to 2 mg/cm2 of carbon. In order to assure that the catalyst layer was completely penetrated by the electrolyte each electrode was initially immersed under vacuum in isopropanol for an hour and then in water overnight prior to use in the electrochemical cell.

The electrodes were evaluated for their activity for methanol oxidation in sulfuric acid at 60°C. This condition was selected because of the very large body of previous work in which other catalysts have been evaluated at the same condition, e.g. (17). Tests at this condition can differentiate candidate catalysts: platinum-ruthenium in alloys, with about 1/1 atom ratio, which are the most active catalysts in sulfuric acid at 60°C also prove to be the most active catalysts in perfluorosulfonic acid membrane fuel cells at 80°C.

For the electrochemical measurements a standard three chamber cell was constructed with a Luggin capillary connecting to a hydrogen reference electrode, in the same electrolyte as the working electrode, 1.5 M H_2SO_4. The working electrode, a 1 cm^2 tab, was held in place by gold wire. The cell was heated by immersion in a water thermostated water bath.

4. Experimental Results (J.A.S. Bett, A.J. Aldykiewicz)

An initial measurement was made of the activity of a commercial platinum-ruthenium catalyst to validate the test procedures. Figure 1 shows a polarization curve determined for FCA-7X, obtained from Johnson Matthey. The catalyst contained a 20% of noble metal, 50/50 atom percent PtRu, supported on carbon black.

Current density has been expressed as mA/mg platinum so that the activity might be compared with that of a similar 50/50 atom percent PtRu catalyst reported by Watanabe (20). The figure shows that the activity of the Johnson Matthey catalyst was close to that of the Watanabe catalyst. It is possible that the more pronounced curvature at higher current density in the Watanabe measurements might result from mass transfer limits set in the much thicker electrode, 2.0 mg/cm^2 Pt, of Watanabe. The measurement clearly differentiates the more active PtRu from the lower activity of pure platinum.

Initial experiments in the preparation of metal macrocyclic catalysts have been performed with cobalt and nickel phthalocyanine because they were first available. The intent was to prepare catalysts in which the macrocycles were adsorbed as monolayers on carbon. The adsorption of cobalt phthalocyanine on various carbons have been shown to follow Langmuir isotherms, establishing a monolayer when the solution concentration was greater than about 10 mg/L (1.75×10^{-5} M) (3).

For the present catalysts, the macrocycles were dissolved in pyridine and slurried with Vulcan XC-72 carbon. The concentrations in the initial solutions were sufficient to deposit a monolayer on 0.5 g of Vulcan XC-72 from 500 ml of pyridine so that the residual concentration in solution, in the equilibrated slurry, exceeded 10 mg/L, i.e. the monolayer region of the isotherm.

The adsorption was followed by measurement of the visible spectrum of the pyridine solution before and after addition of carbon. For both cobalt and nickel phthalocyanines there was a pronounced decrease in the intensity of color following adsorption and this was confirmed by the spectra shown in figure 2 for cobalt phthalocyanine. Using the decrease in the Soret band at a wavelength of about 320 nm, the concentration of phthalocyanine on the carbon surface was calculated, by difference, to be 0.03 g/g carbon for CoPC and 0.015 g/g for NiPC. The surface area of Vulcan XC-72 was 240 m^2/g so the area occupied by each molecule of Co and Ni phthalocyanine was 380 and 760 nm^2/molecule, respectively. This value is close to the range of 600 to 800 nm^2/molecule determined for adsorption on high surface area carbons (3). Yeager et al. have measured a value of 550 nm^2/molecule for tetrasulfonate phthalocyanines adsorbed on graphite (6).

After adsorption, the carbon was separated from the solution and dried at 100°C. The dried powder was then prepared in electrodes for electrochemical evaluation. Figures 3 and 4 show cyclic voltammograms for the adsorbed nickel and cobalt phthalocyanines in pure sulfuric acid.

These show well defined reversible couples at about 875 mv for NiPC and 950 mv for CoPC. Both voltammograms appear very similar to voltammograms reported by Yeager et al. for cobalt tetrasulfonate phthalocyanine adsorbed on graphite (6) and by Van der Putten et al. (13) for CoPC adsorbed on pyrolytic graphite, for which the redox potential was also 950 mv.

The peak current of the redox couples were directly proportional to sweep rate as would be expected from charge transfer to a species adsorbed on the carbon surface. Since Van der Putten et al. found that the potential of the couple was independent of potential they assigned the couple to the reaction:

$$[LCo^{III}OH_2]^{+3} + e \quad <-> \quad [LCo^{II}OH_2]^{+2}$$

rather than:

$$[LCo^{III}OH]^{+2} + H^{+} + e \quad <-> \quad [LCo^{II}OH_2]^{+2}$$

From the area under the peak the charge associated with the couple could be calculated. This gave a value for the loading of phthalocyanine of 0.009 g/g carbon for CoPC, to be compared to the value calculated from the solution adsorption spectra of 0.03 g/g.

For NiPC, assuming by analogy with CoPC that the redox couple was associated with $Ni^{2+/3+}$, the coverage from the voltammetry was 0.010 g/g to be compared with 0.015 g/g from the solution adsorption spectra.

Thus, for both CoPC and NiPC the values for the coverage calculated from the voltammetry were lower than those obtained from the initial adsorption procedures. The difference appeared to be caused by incomplete wetting of the catalyst by electrolyte, despite the extensive pre-wetting procedures used, since the double layer charging current in flat region of the voltammogram was lower than that calculated from the double layer capacitance of carbon and the surface area of carbon in the electrode. Further experiments with varied loadings of catalyst will be required to establish the cause.

In both the CoPC and NiPC voltammograms there was a feature at about 0 V that appeared to have the characteristics of hydrogen evolution and oxidation. Van der Putten et al. reported a similar feature for CoPC which they associated to the couple $Co^{+1/+2}$. However, subsequent tests with the gold wire holder showed that it gave rise to a small current as an artifact.

After the initial voltammograms in pure 1.5 M H_2SO_4, methanol was added to the electrolyte at a concentration of 1.0 M. For both NiPC and CoPC, there was no evidence of additional current due to methanol oxidation when the voltammetric cycles were repeated. This was not unexpected in the absence of platinum co-catalyst. Preparation of catalysts are in progress in which carbon with monolayers of the metal macrocycles will be impregnated with platinum to explore the possibility for co-catalysis.

5. References

(1) S. Sarangapani, S. Sarangapani and B. Morriseau, Electrochemical Soc. Mtg., Abstract 476, Lake Tahoe, 1995

(2) Y-K Lai and K-Y Wong, Electrochemica Acta, 38 (1993) 1015

(3) J. Bett, W. Vogel, K. Routsis and S. Anderson, Am. Chem Soc. 6th Biennial Fuel Symposium, New York, Sept. 1969.

(4) J. Bett, H. Kunz, S, Smith and L. Van Dine, Final Report, Los Alamos National Laboratory, SubContract No 9-X-13-D6271-1, 1984.

(5) D. Scherson, A. Gupta, S. Fierro, E. Yeager, E. Kordesh, m. Eldridge, J. Hoffman and H. Blue, Electrochemica Acta, 28 (1983) 1205

(6) J. Zagal, P. Bindra and E. Yeager, J. Electroanal. Chem., 127 (1980) 1506

(7) R. Durand and F. Anson, J. Electroanal. Chem., 134 (1982) 273

(8) H. Gasteiger, N. Markovic, P. Ross and E. Cairns, J. Electrochem. Soc., 141 (1994) 1795

(9) K. Kadish, M. Morrison, L. Constant, L. Dickens and D. Davis, J. Am. Chem. Soc. 98 (1976) 8387

(10) K. Kadish, J. Electroanal. Chem., 168 (1977) 261

(11) L. Bottomley and K. Kadish, Inorg. Chem. 20 (1981) 1348

(12) J. Manassen and A. Bar-Ilan, J. Catalysis, 17 (1970) 86

(13) A. Van der Putten, A. Elzing, W. Visscher and E. Barendrecht, J. Electroanal. Chem., 221 (1987) 95

(14) A. Bettelheim, R. Chan and T. Kuwana, J. Electroanal. Chem., 49 (1987) 391

(15) M. Yamana, R. Darby and R. White, Electrochemica Acta, 29 (1984) 329

(16) N. Kobayashi and Y. Nashimya, J. Electroanal. Chem., 181 (1984) 107

(17) C.-M. Che and C.-K. Poon, Pur Appl. Chem., 60 (1988) 495

(18) M. Schröder, Pure Appl. Chem., 60 (1988) 517

(19) C.-M. Che, K.-Y. Wong, and C.-K. Poon, Inorg. Chem., 25 (1986) 1809

(20) M. Watanabe, M. Uchida and S. Motoo, J. Electroanal. Chem., 229 (1987) 395

(21) J. Zagal, R. Sen and E. Yeager, J. Electroanal. Chem., 83 (1977) 207

(22) R. Durand and F. Anson, J. Electroanal. Chem., 134 (1982) 273

(23) C-M Che, K-Y Wong,W-O Lee and F. Anson, J. Electroanal. Chem., 309 (1991) 303

(24) M. Pourbaix, Atlas of Electrochemical Equilibria, Guathier-Villars, Paris, 1963

(25) A. Brown and F. Anson, J. Electroanal. Chem., 83 (1977) 203

(26) A Bettelheim, D. Ozer,R. Harth and R. Murray, J. Electroanal. Chem., 246 (1988) 139

TABLE 1

CATION REDOX POTENTIALS IN PORPHYRINS AND PHTHALOCYANINES

Metal Complex	State	Redox Potential Vs SHE	Reference
Cobalt $Co^{2+/3+}$			
$Co^{2+/3+}$	dissolved	1.80	(24)
Phthalocyanine(PC)	dissolved	1.01	(12)
Phthalocyanine	ads. on graphite	0.95	(13)
TetrasulfonatoPC	ads. on graphite	1.04	(6)
Tphenylporphyrin(P)	dissolved	0.76	(12)
Tpyridylporphyrin	dissolved	0.15	(14)
Tpyridylporphyrin	ads. on carbon	0.10	(14)
Tpyridylporphyrin	ads. on carbon	0.40	(14)
Methylethyl-ethyl propanoateporphyrin	ads. on graphite	0.79	(7)
Iron $Fe^{2+/3+}$			
$Fe^{2+/3+}$	dissolved	0.77	(24)
Phthalocyanine(PC)	dissolved	0.40	(12)
Phthalocyanine	ads. on graphite	0.65	(13)
Cl_4PC	att. on carbon		
	H/T 200°C	0.63	(15)
	H/T 600°C	0.54	(15)
TetrasulfonatoPC	ads. on graphite	0.64	(6)
mesoTphenylporphyrin	ads. on graphite	0.04	(16)
mesomaminophenylP	ads. on graphite	0.08	(16)
mesoTmaminophenylP	ads. on graphite	0.13	(16)
Ruthenium $Ru^{2+/3+}$			
$Ru^{2+/3+}$	dissolved/oxide	1.30	(24)
$ToNH_2phenylP(CH_3CN)_2$	ads. on carbon	0.35	(26)
$[(bpy)_2(OH)_2]^{2+}$	dissolved	0.88	(23)
$cis[Ru^{II}LClH_2O)$	ads. on carbon	0.47	(2)
$[arylpyridyl(NH_3)_5]^{2+}$	ads. on graphite	0.31	(25)

TABLE 2

METAL MACROCYCLIC COMPLEXES SELECTED FOR EVALUATION

COMPLEX	SOURCE
Phthalocyanines, Fe,Co, Ni, Sn	Aldrich
Tetramethoxyphenyl porphyrins V, Fe, Co, Mo, Ru, Sn	Porphyrin Products, Logan, Utah
Tetramethyl-tetraaza-cyclotetradecane, Co, Ru	U. Connecticut

Figure 1

Comparison of Methanol Oxidation Activity of Johnson Matthey and Watanabe PtRu Catalysts

1.5M H_2SO_4, 1M CH_3OH, 60°C

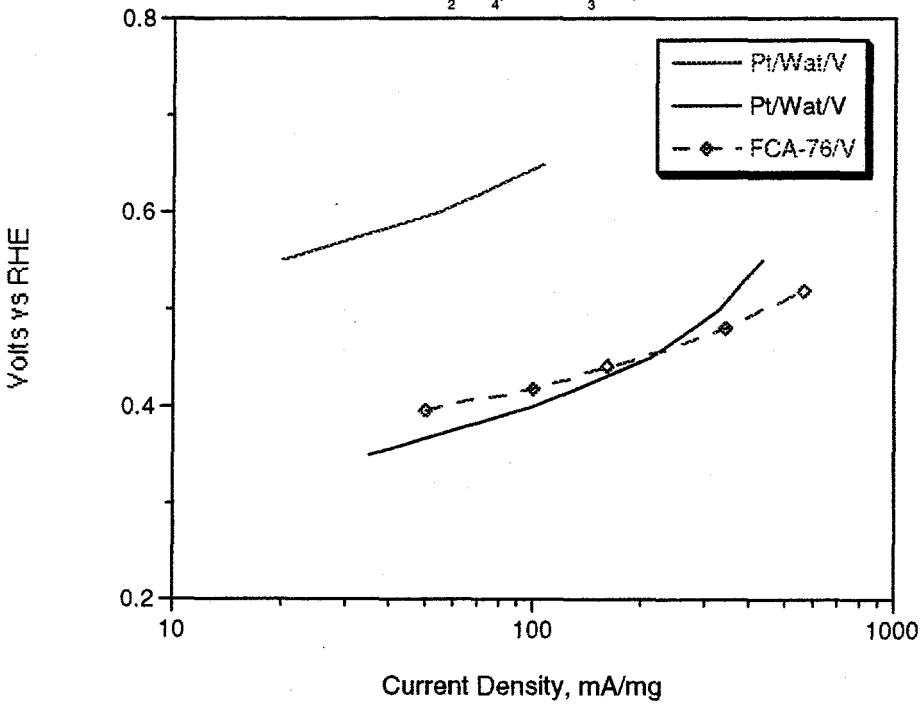

Figure 2

Visible absorption spectrum of cobalt phthalocyanine solution before and after adsorption on Vulcan XC-72

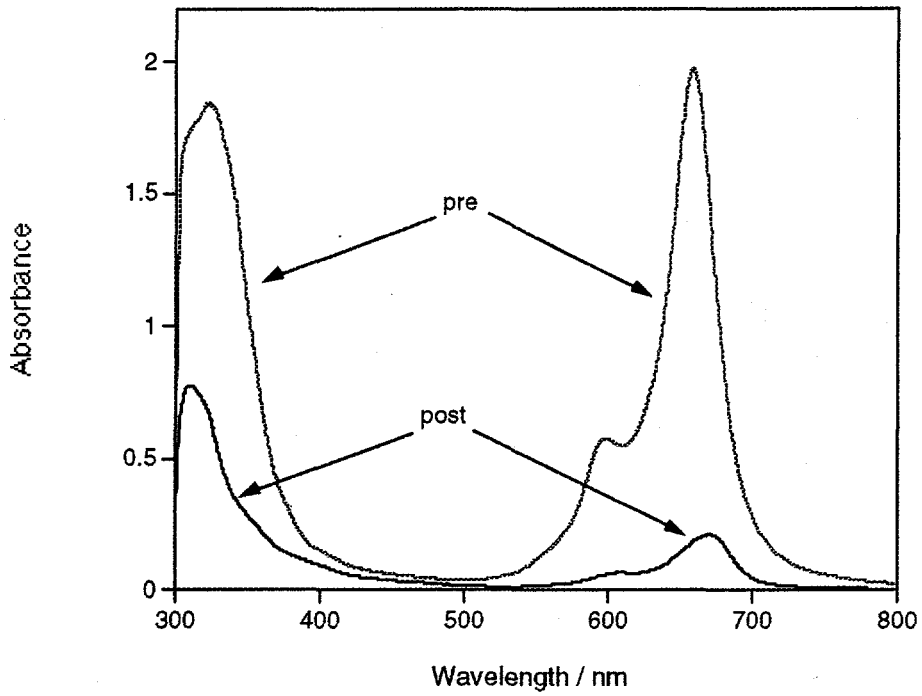

Figure 3

Cyclic voltammogram of cobalt phthalocyanine adsorbed on Vulcan XC-72
1.5M H_2SO_4, 60°C, 100mV/sec

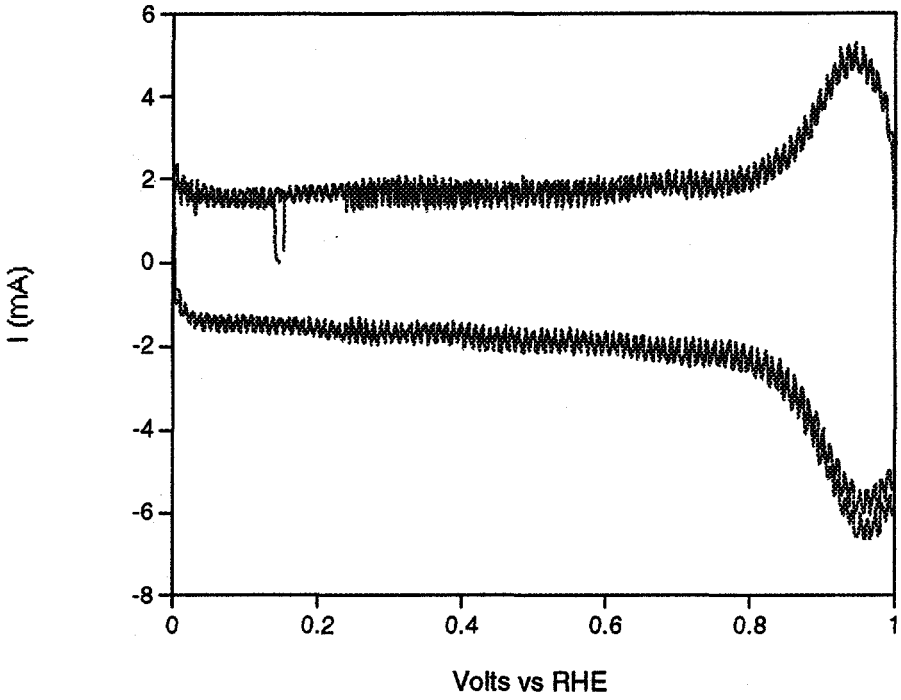

Figure 4

Cyclic voltammogram of nickel phthalocyanine adsorbed on Vulcan XC-72

1.5M H_2SO_4, 60°C, 100 mV/sec

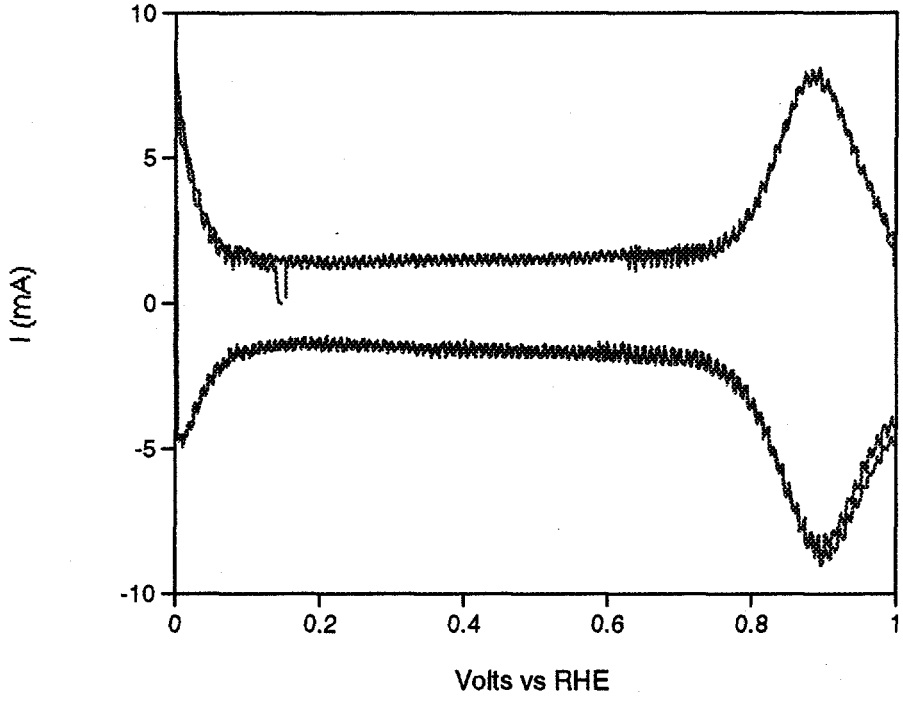

B. Task 2.0: Physically Modified Proton Exchange Membrane

1. Summary

A Nafion membrane of uniform 5 mil. thickness was successfully fabricated in the laboratory. A commercial and the prepared Nafion membranes were characterized by XRD and FTIR in addition to acid titration. The prepared membrane has similar characteristics to the commercial membrane; however, the commercial membrane is more crystalline than the prepared membrane. A membrane methanol transport apparatus was designed, assembled and tested. Methanol transport rates through a commercial Nafion 117 membrane were measured at room temperature. A mathematical model for methanol transport rate was developed and applied to determine the methanol diffusion coefficient. Results shows that the measured diffusion coefficient is comparable to the data in literature.

2. Introduction

The polymeric electrolyte that is currently most frequently used is Nafion(R) 117, a perfluorosulfonic acid membrane manufactured by DuPont. Although much research has been done to measure fundamental properties of this solid polymeric electrolyte (1), much is still unknown about its structure.

The structure of Nafion consists of long chain fluorinated carbon regions, similar to Teflon, but with periodic pendant groups containing sulfonic acid (2). Nafion is fabricated from a copolymer of tetrafluoroethylene and a vinyl sulfonyl fluoride that is converted into acid form. Similar polymeric electrolytes with different pendant groups are manufactured by DOW, Asahi Chemical and Chlorine Engineers. When in the form of a membrane, the PEM can be thought to consist of two regions, a hydrophobic region similar to Teflon and small hydrophilic regions containing the sulfonic acid groups, protons, and water (3). A third intermediate region has also been identified. The hydrophilic regions may have a periodic variation in cross-sectional area. Considerable research has been done to determine this structure and its properties.

Early cells using solid polymeric electrolytes were fabricated by pressing the anode and cathode onto the opposite surfaces of the membrane. Both of these electrodes were porous mixtures of platinum black and Teflon. Since all of the catalyst was not in contact with electrolyte, this method of cell fabrication resulted in only the

regions of the electrodes near the polymeric membrane being electrochemically active (4).

More recently, a form of the polymeric electrolyte dissolved in ethanol has been used to coat the catalyst (5). This process has resulted in cell performance increases and the ability to use much lower loadings of platinum catalyst supported on carbon.

When Nafion is adsorbed on a platinum catalyst, the potentiometric determination of hydrogen oxidation indicates that almost all of the platinum surface atoms are active. This implies a restructuring of the polymer to provide sulfonic acid groups to the surface platinum atoms (4).

Another possible surface effect has been found in experiments to determine the equilibrium water content of Nafion. This content was found to be less when water vapor was used for equilibration than when liquid water of the same activity was used (1). A difference in surface structure between contact with vapor and liquid could explain this difference in water absorption. Differences in the contact angle of water on the membrane have been measured for membranes previously exposed to liquid water or water vapor (6).

A restructuring of the Nafion has also been used to explain enhanced diffusion through Nafion that was impregnated into the pores of a polycarbonate membrane (7). The maximum enhancement for the diffusion of the ion $Ru(bpy)_3^{3+}$ was found to occur for a pore diameter of 45 nm. Improvements in diffusion rates have also been observed when the Nafion is impregnated in a porous Teflon membrane (8). The pore size at which this enhancement occurs is of the order of the structure of the hydrophilic and hydrophobic regions in bulk Nafion. The small pores are therefore thought to modify this structure and change the polymer's properties. The enhanced flux rates are thought to be an effect of surface diffusion (9). Surface effects that enhance the conductivity of composites have been observed in other cases (10). An optimum pore diameter of 1 to 5μm has been found for the conductivity of composite membranes using Teflon as the support (11).

The change in the structure of Nafion in small pores may be beneficial with respect to the transport of methanol through the Nafion. Experiments have shown that the relative transport rates of gaseous methanol and water through a porous silica-alumina membrane can be changed by adjusting the pore size of the membrane (12). Methanol transport rates less than 10% of that for water were

obtained using membranes with fine pore structures. The small pores are thought to resist the migration of the larger methanol molecules somewhat like molecular sieving. The sieving is thought to occur for pore diameters in the range of 0.9 to 14 nm depending on the specie adsorbed on the walls of the pores. The diffusion of methanol through Nafion might be expected, therefore, to depend on the size of the pores in which the Nafion is impregnated. Some success in increasing the performance of direct methanol fuel cells by using Nafion incorporated in a composite structure has been reported (13).

Considerable modeling has been conducted on the membrane and electrodes of PEM fuel cells (14 to 20). These models have accounted for the bulk properties of the membrane with suitable accounting for the effect of water content and the electroosmotic drag of water through the membrane. These models assumed that the electrolyte is homogeneous. None of these models have considered the restructuring of the membrane at its interfaces with electrode materials.

Since the work on the conductivity of composite membranes using a perfluorosulfonic acid indicate that ionic migration along the surface of the electrolyte may be important, further work on the development of electrode models is needed in order to optimize electrode structures. The optimum manner in which catalyst should be distributed within an electrode may be significantly affected by such an assumption depending on the properties of the catalyst.

3. Membrane Fabrication (C. He, J.-C. Lin)

a. Membrane Materials

In this work, a variety of composite membranes are being prepared by impregnating Nafion solution into porous membranes having different pore sizes. Fine materials such as aluminum oxide, silicon carbide, and Teflon, will be mixed with Nafion solution and then will be cast as membranes. Fine powders, colloids, and porous membranes available in the laboratory are shown in Tables 1, 2 and 3, respectively.

b. Membrane Casting

Initial trials were performed in the laboratory to evaluate the properties of a pure Nafion membrane cast from a Nafion solution. Membranes were typically prepared by mixing 60 mL 5 % Nafion

solution and 30 mL dimethyl sulfoxide (DMSO) solvent in a specially designed flat glass membrane fabrication cell. The procedure involved heating the solution at 90 ^{o}C for two hours to evaporate the alcohol inside a forced convection oven. In order to remove DMSO solvent, temperature was raised to 180 ^{o}C for another one hour and then cooled down to the room temperature. The resulting deposited membrane was peeled off from the flat glass by wetting the membrane with 1:1 ethanol/water solution. The thickness of Nafion was approximately 5 mil as measured by a micrometer.

4. Characterization (J.-C. Lin)

a. Determination of Equivalent Weight

Equivalent weights of various membranes were determined by the titration method whereby 0.2 g dry membrane was submerged into 10 mL of 1 M sodium chloride solution in order to exchange the protons from the membrane. Sodium hydroxide (0.01 N) was used to titrate the solution with phenolphthalein as an indicator. Typical results showed the equivalent weight of commercial Nafion 117 membrane was about 1170 g/mole.

b. X-ray Diffraction

A Scintag X-ray diffractometer (XRD) 2000^{TM} was used to identify the crystalline structure of the membranes. XRD data for commercial Nafion 117 and prepared Nafion membrane are shown in Figures 1a and 1b. A sharp peak appeared at $2\theta \approx 17.7^{o}$ for the commercial membrane (Figure 1a) associated with the crystallinity of the membrane. The prepared Nafion membrane (Figure 1b) did not show any sharp peaks in the XRD data. This indicates that the prepared membrane was less oriented than the commercial Nafion membrane. The difference in crystallinity between commercial and prepared membranes may have been due to different preparation processes.

XRD data for 0.22 μm pore size hydrophilic polyvinylidene fluoride (PVF) membrane that will be used as the filler of composite membranes are shown in Figure 2. Results indicate that there is a sharp peak appearing at $2\ \theta \approx 20^{o}$ which suggests PVF membrane is highly crystalline.

c. Fourier Transform Infrared Spectroscopy

Fourier Transform Infrared (FTIR) spectroscopy was conducted using a Nicolet magna-IR^{TM} 750 spectrometer. Diffuse reflectance infrared spectra for commercial Nafion 117 and prepared Nafion membrane are presented in Figures 3 (a) and (b). A diffuse reflectance infrared spectrum for PVF membrane is shown in Figure 4.

Infrared spectrum of the acid form of Nafion membrane has been studied extensively (21-22). Previous work indicates that the water content will affect the absorbance of the membrane. Figure 3 shows that the prepared membrane has stronger absorbance than commercial membrane at approximately 3700 cm^{-1} which is assigned to hydrogen bonding of the water. This indicates that the prepared membrane has higher water content than commercial membrane under dry conditions. The particular peak appearing at approximately 3950 cm^{-1} may be due to the interaction between the residual DMSO solvent and Nafion membrane.

The diffuse reflectance spectrum for PVF shows a broad peak appearing between 3200 cm^{-1} and 3600 cm^{-1} which is assigned to water. The peaks at approximately 3000 cm^{-1} and 1450 cm^{-1} are attributed to the CH_2 groups. Peaks for CF_2 groups can been found throughout range. A strong peak at 1730 cm^{-1} is assigned as the C=C groups, and this does not disappear when the membrane is boiled in doubly distilled water or washed with methylene chloride. This unsaturated bonding in the commercial PVF membrane may be the result of the electron beam which is used to create the pores of the membrane.

d. Membrane Ionic Conductivity Measurements

The methanol transport apparatus (described in detail below) has been designed to allow for simultaneous measurement of methanol transport and membrane conductivity. A Solartron Frequency Response Analyser has been ordered for the conductivity measurement. This capability is expected to be operational in the near future.

5. Methanol Transport (M.B. Cutlip, J.-C. Lin)

a. Experimental

Methanol transport rates through Nafion 117 membrane are being measured in a specially designed membrane transport apparatus with a membrane support cell. In the tests performed this quarter, , the membrane was submerged in deionized distilled water (DDW) overnight before installation of the membrane into the cell. The schematic diagram of experimental setup is shown in Figure 5. Typically, liquid methanol and water mixtures were fed to one side of the single cell. Nitrogen and water vapor mixtures were introduced to the other side of the cell. The membrane is supported on both sides by a Toray carbon paper substrate. In order to eliminate the boundary layer resistance in the gas phase and obtain a uniform methanol concentration over the entire channel, a recycle pump was used on the gas side.

Steady state methanol concentrations in the gas phase effluent were measured by gas chromatography using a six foot Hay-Sep R column and a thermal conductivity detector. The oven temperature and flow rate were 130 ^{o}C and 30 mL/min., respectively.

b. Model Development

The schematic diagram of methanol transport mechanism through the membrane is presented in Figure 6. On the liquid side, methanol diffuses through the liquid boundary layer and carbon substrate, reaches the equilibrium with the methanol at the interface, and then diffuses through the interior of the membrane. On the gas side, methanol at the interface is in equilibrium with the gas phase methanol and subsequently diffuses into the bulk gas through another carbon substrate and the gas boundary layer.

A simple model for methanol transport was developed based on the following assumptions:

1. The carbon paper supporting the membrane is extremely porous, i.e. there is no resistance to mass transport which is due to the carbon paper.

2. Equilibrium is achieved at interfaces.

3. The partition coefficients (concentration in membrane /concentration in liquid phase) for methanol are constant and independent of concentration.

The relationship for equilibria are described by

$$k_{e,1} = \frac{[CH_3OH]_l^{\langle I \rangle}}{[CH_3OH]_l^{\langle I, m \rangle}} \quad (1)$$

$$k_{e,g} = \frac{[CH_3OH]_g^{\langle II \rangle}}{[CH_3OH]_l^{\langle II, m \rangle}} \quad (2)$$

where $k_{e,1}$ and $k_{e,g}$ are the partition coefficients between two phases.

Methanol flux through liquid boundary layer, membrane, and gas boundary layer can be presented by equations (3) to (5), respectively.

$$J_l = \frac{k_1 \bullet D_{CH_3OH}^{\langle l \rangle}}{\delta_1} \left([CH_3OH]_l - [CH_3OH]_l^{\langle I \rangle} \right) \quad (3)$$

$$J_m = \frac{\varepsilon \bullet D_{CH_3OH}^{\langle l \rangle} \bullet \lambda}{L \bullet \tau} \left([CH_3OH]_l^{\langle I, m \rangle} - [CH_3OH]_l^{\langle II, m \rangle} \right)$$

$$= \frac{D_{CH_3OH}^{\langle m \rangle}}{L} \left([CH_3OH]_l^{\langle I, m \rangle} - [CH_3OH]_l^{\langle II, m \rangle} \right) \quad (4)$$

$$J_g = \frac{k_2 \bullet D_{CH_3OH}^{\langle g \rangle}}{\delta_2} \left([CH_3OH]_g^{\langle II \rangle} - [CH_3OH]_g \right) \quad (5)$$

where

k_1, k_2= correction factor for non-homogeneous interface

ε= porosity

τ= tortuosity

λ= correction factor for interaction between membrane and methanol

L= membrane thickness

δ= boundary layer

D= diffusion coefficient

Combining equations (1)to(5) allows the methanol flux through membrane to be expressed as

$$J_m = \frac{D^{\langle m \rangle}_{CH_3OH}}{L}\left(\frac{[CH_3OH]_l}{k_{e,l}} - \frac{J_l \bullet \delta_1}{k_1 \bullet D^{\langle l \rangle}_{CH_3OH} \bullet k_{e,l}} - \frac{[CH_3OH]_g}{k_{e,g}} - \frac{J_g \bullet \delta_2}{k_2 \bullet D^{\langle g \rangle}_{CH_3OH} \bullet k_{e,g}}\right) \quad (6)$$

At steady state, $J_o = J_m = J_g = J_l$, therefore, methanol flux can be expressed as

$$J_o = \frac{\frac{D^{\langle m \rangle}_{CH_3OH}}{L}\left(\frac{[CH_3OH]_l}{k_{e,l}} - \frac{[CH_3OH]_g}{k_{e,g}}\right)}{1 + \frac{D^{\langle m \rangle}_{CH_3OH} \bullet \delta_1}{L \bullet k_1 \bullet k_{e,l} \bullet D^{\langle l \rangle}_{CH_3OH}} + \frac{D^{\langle m \rangle}_{CH_3OH} \bullet \delta_2}{L \bullet k_2 \bullet k_{e,g} \bullet D^{l}_{CH_3OH}}} \quad (7)$$

Experimental results showed that variation of liquid flow rate and the gas side recycle ratio did not affect the methanol flux, i.e., the resistance of membrane dominated the methanol transport process. Therefore, the methanol flux equation can be simplified to

$$J_o = \frac{D^{\langle m \rangle}_{CH_3OH}}{L}\left(\frac{[CH_3OH]_l}{k_{e,l}} - \frac{[CH_3OH]_g}{k_{e,g}}\right) \quad (8)$$

c. Experimental Results

Methanol flux versus gas phase concentration plots for Nafion membrane using various methanol concentrations at 18 °C are shown in Figures 7-9. Equation 6 shows that the apparent effective diffusion coefficient, $D^{\langle m \rangle}_{CH_3OH} / k_{e,l}$, can be obtained from the intercept of the plots on the ordinates. The results are summarized in Table 4. A more extensive estimate for the effective diffusion coefficient was performed using nonlinear regression with POLYMATH (23) with all of the experimental data for a constant partition coefficient of 5.0 as determined by Xiaoming et al. (24). This estimated diffusion coefficient is compared with the result of Xiaoming et al. (24) in Table 5 where quite satisfactory agreement is indicated for the commercial Nafion 117 measurements.

6. References

(1). T. A. Zawodzinski, T. E. Springer, J. Davey, J. Valerio, and S. Gottesfeld, "Water Transport Properties of Fuel Cell Ionomers", The Electrochemical Society, 91-10, pp. 187-196 (1991).

(2). W. Grot, "Perfluorinated Ion Exchange Membranes of High Chemical and Thermal Stability", Chem. Ing. Tech., 44, pp. 167 (1972).

(3). W. Y. Hsu and W. T. Gierke, J. Mem. Sci., 13 (1983).

(4). K. Mootz and J.A.S. Bett, "The Activity of Platinum Black for Oxygen Reduction in Proton Exchange Membrane (Nafion) Fuel Cells", The Electrochemical Society, 90-2, Abstact No. 122, pp. 183 (1990).

(5). S. Srinivasan, E.A. Ticianelli, C.R. Derouin, and A. Redondo, "Advances in Solid Polymer Electrolyte Fuel Cell Technology with Low Platinum Loading Electrodes", Journal of Power Sources, 22, pp. 359-375 (1988).

(6). T. A. Zawodzinski, Jr., S. Gottesfeld, S. Soichet, and T. J. McCarthy, "The Contact Angle on Ferfluorosulfonic Acid Membranes", Short Communication, Journal of Applied Electrochemistry, 23, pp. 86-88 (1993).

(7). J. Leddy and N. E. Vanderborgh, "Microstructural Enhancement of Mass Trtansport Through Nafion-Nuclepore Composite Membranes", J. Electroanal. Chem., 235, pp. 299-315 (1987).

(8). R. M. Penner and C. R. Martin, "Ion Transporting Composite Membranes", J. Electrochem. Soc. 132, pp. 514-515 (1985).

(9). J. Leddy and L. Zook, "Composite Ion Exchange Materials: Flux Enhancements Through Microbead Composites", The Electrochemical Society, Extended Abstracts, 93-1, Abstract No. 1821, pp. 2479 (1993).

(10). J. B. Wagner, Jr., "Composite Conductors", The Electrochemical Society Proceedings Vol. 87-3, Electrochemistry and Solid State Science Education at the Graduate and Undergraduate Level, pp. 110-115 (1987).

(11). E. J. Taylor, C. Pazienza, R. Waterhouse, and G. Wilemski, "The Effect of Support Morphology on Composite Membrane Performance", The Electrochemical Society, 86-2, Abstract No. 590, pp. 883-884 (1986).

(12). M. Asaeda, L. D. Du, and M. Fuji, "Separation of Alcohol/Water Gaseous Mixtures by an Improved Ceramic Membrane", Journal of Chemical Engineering of Japan, 19, pp. 84-85 (1986).

(13). T. A. Zawodzinski, Jr., T. E. Springer, M. S. Wilson, and S. Gottesfeld, "Methanol Cross-over in DMFC's: Development of Strategies for Minimization", The Electrochemical Society, Proceedings Vol. 94-2, Abstract no. 613, pp. 960 (1994).

(14). D. M. Bernardi and M. W. Verbrugge, "Mathematical Model of a Gas Diffusion Electrode Bonded to a Polymer Electrolyte", AIChE Journal, Vol. 37, No. 8, pp. 1151-1163 (1991).

(15). T. F. Fuller and J. Newman, "Water and Thermal Management in Solid-Polymer-Electrolyte Fuel Cells", Journal of the Electrochemical Society, Vol. 140, pp. 1218-1225 (1993).

(16). J. Leddy, A. E. Iverson, N. E. Vanderborgh, "Modeling of the Electrode/Ionomer Interface in a Solid Polymer Electrolyte Fuel Cell", The Electrochemical Society, Vol. 86-2, Abstract No. 134, pp. 196 (1986).

(17). W. Paik, T, J. Springer, and S. Srinivasan, "Kinetics of Fuel Cell Reactions at the Platinum/Solid Polymer Electrolyte Interface", Journal of the Electrochemical Society, Vol. 136, No. 3, pp. 644-649 (1989).

(18). T. E. Springer, M. S. Wilson, and S. Gottesfeld, "Modeling and Experimental Diagnostics in Polymer Electrolyte Fuel Cells", Journal of the Electrochemical Society, Vol. 14, No. 12, pp. 3513-3526 (1993).

(19). J. Wang and R. F. Savinell, "Modeling Study of Electrode Structure Effects on Performance of Methanol Electrodes", The Electrochemical Society, Vol. 94-1, Abstract No. 629, pp. 1000 (1994).

(20). R. Zhang and J. M. Fenton, "Mathematical Modeling of Electrode Processes in a PEM Fuel Cell", The Electrochemical Society, Vol. 92-2, Abstract No. 88, pp. 140 (1992).

(21). M. Lopez, B. Kipling, and H.L. Yeager, *Anal. Chem.*, **48**, 1120 (1976).

(22). C. Heitner-Wirguin, *Polymer*, **20**, 371 (1979).

(23). M. Shacham, and M.B. Cutlip, *Polymath 4.0*, CACHE Corporation, Austin, TX (1996).

(24). R. Xiaoming, T.A. Zawodzinski, Jr., H. Dai, and S. Gottesfeld, *The Electrochemical Society*, Extended Abstract, 95-2, Abstract No. 677, pp. 1081-1082 (1995).

Table 1. Powders for Nafion Casting.

Powder	Particle Size	Source
Aluminum Oxide	TBD	Degussa
Silicon Carbide	3 to 0.3 μm	Lonza

Table 2. Colloids for Nafion Casting.

Colloid	Particle Size	Source
EC-TFE Teflon-30 Emulsion	0.2 μm	Electrochem. Inc.
EC-FEP Teflon-120 Emulsion	TBD	Electrochem. Inc.

Table 3 . Porous Membranes for Nafion Impregnation.

Membrane	Pore Size (μm)	Porosity (%)	Thickness (μm)	Source
Polyvinylidene Fluoride (hydrophilic membrane)	0.1	70	125	Millipore
Polyvinylidene Fluoride (hydrophilic membrane)	0.22	70	125	Millipore
Polyvinylidene Fluoride (hydrophilic membrane)	0.45	70	125	Millipore
Polyvinylidene Fluoride (hydrophilic membrane)	0.65	70	125	Millipore
Polyvinylidene Fluoride (hydrophobic membrane)	0.22	75	125	Millipore
Polyvinylidene Fluoride (hydrophobic membrane)	0.45	75	125	Millipore

Table 4. Effect of Concentrations on the Apparent Effective Diffusion Coefficients.

Concentration (M)	Apparent Effective Diffusion Coefficient ($cm^2 \cdot s$) $D^{\langle m \rangle}_{CH_3OH} / k_{e,l}$
0.8	8.3e-7
1.2	7.0e-7
1.6	7.8e-7

Table 5. Comparison of Diffusion Coefficients between This Work and Literature.

Source	Diffusion Coefficient (cm^2/s) at 18 °C
This work	3.8e-6
Xiaoming *et al.**	4.0e-6

* This was calculated from the reported diffusion coefficient at 30 °C and activated energy as presented by Xiaoming et al. (24).

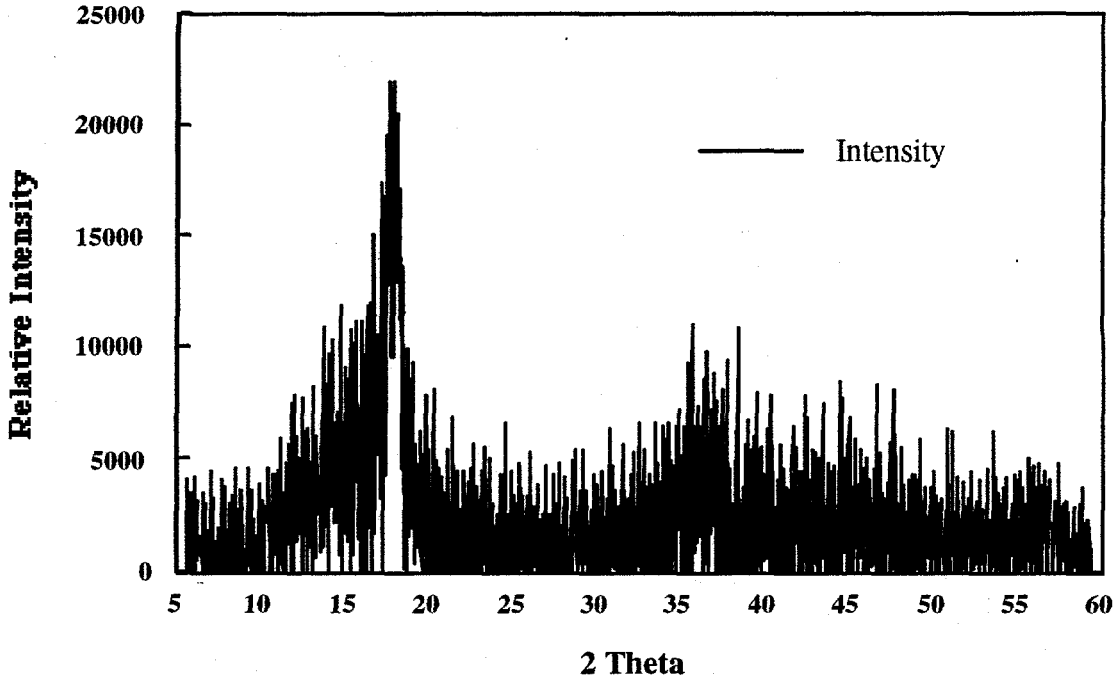

Figure 1a. XRD Data for Commercial Nafion 117 Membrane as Received.

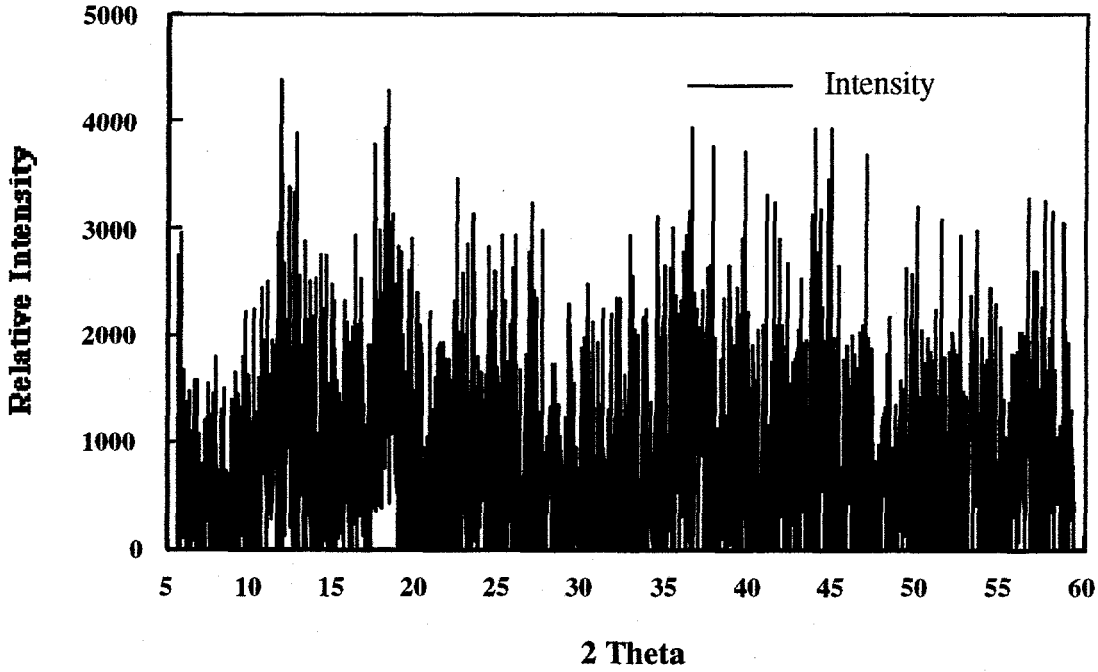

Figure 1b. XRD Data for Prepared Nafion Membrane.

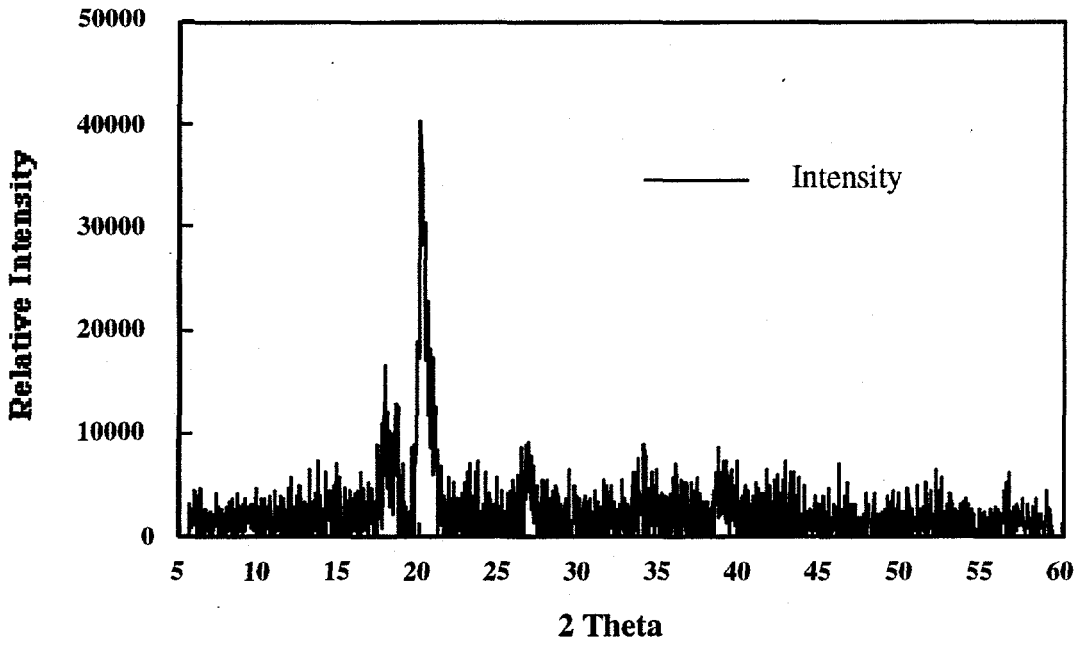

Figure 2. XRD Data for 0.22µm Hydrophilic Polyvinylidene Fluoride Membrane as Received.

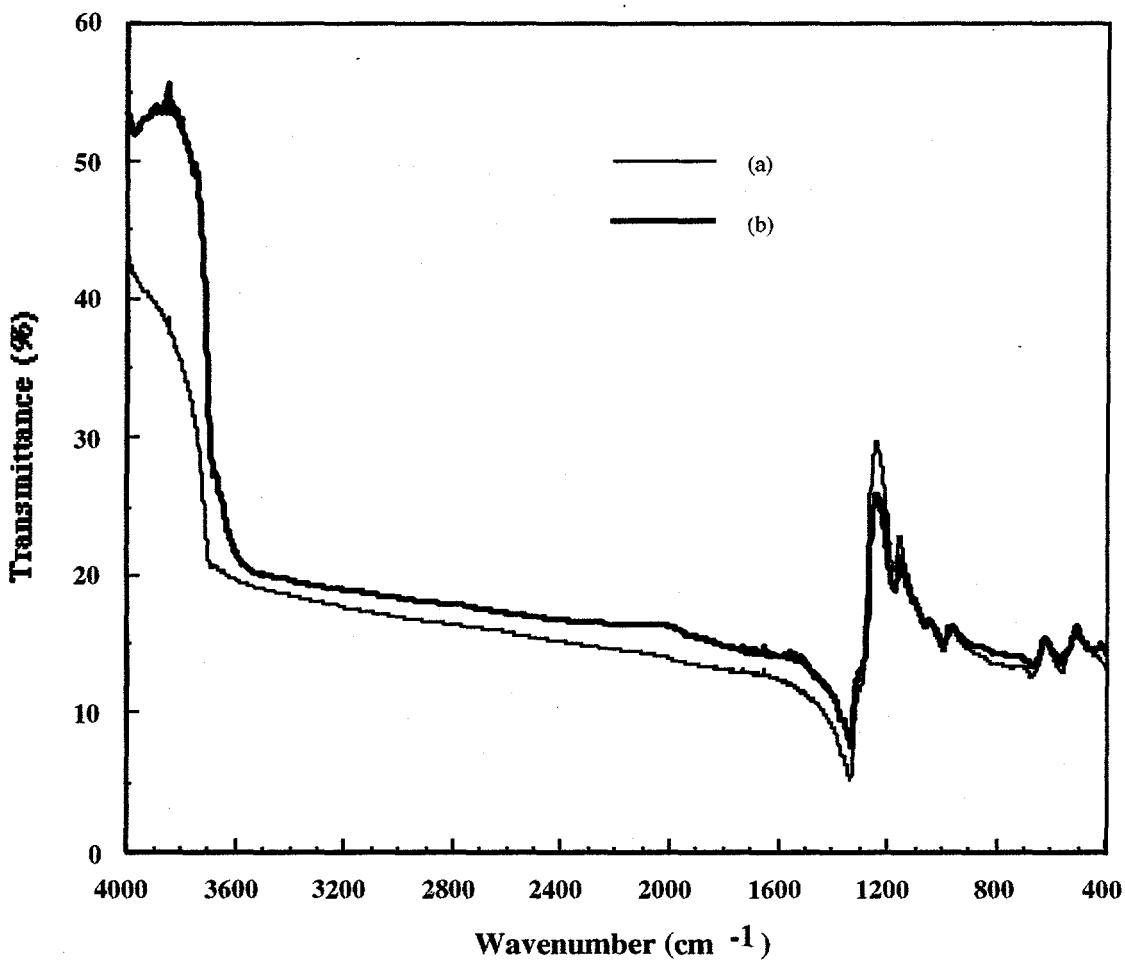

Figure 3. Diffuse Reflectance Infrared Spectra for Commercial Nafion 117 as Received (a) and Prepared Nafion Membrane (b).

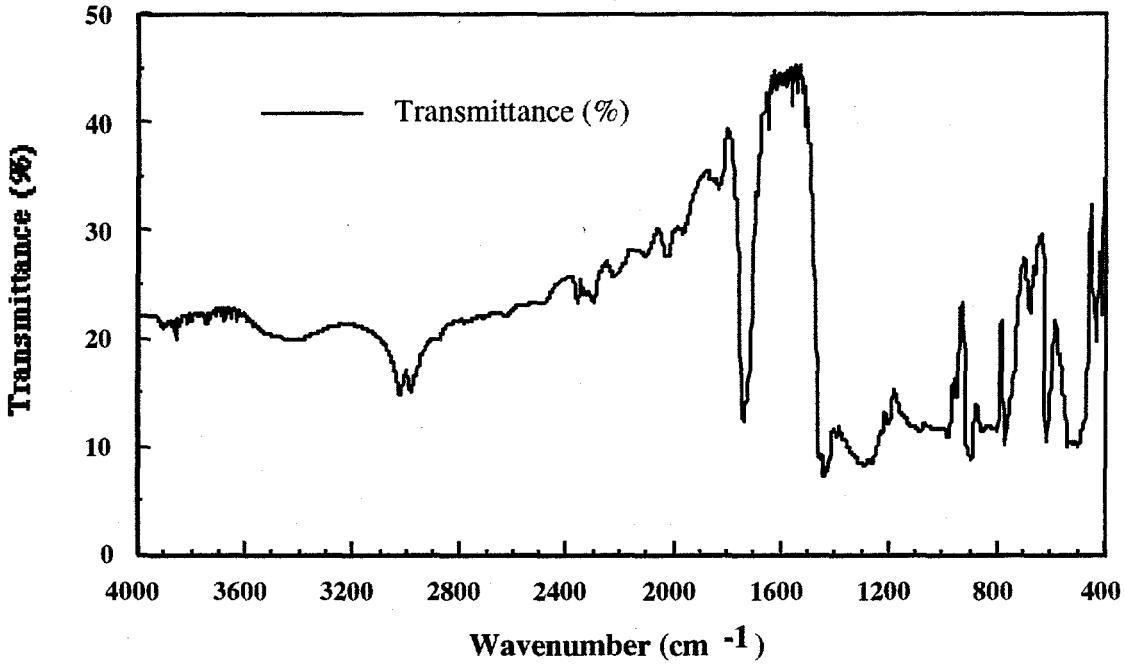

Figure 4. Diffuse Reflectance Infrared Spectrum for 0.22μm Hydrophilic PVF Membrane as Received.

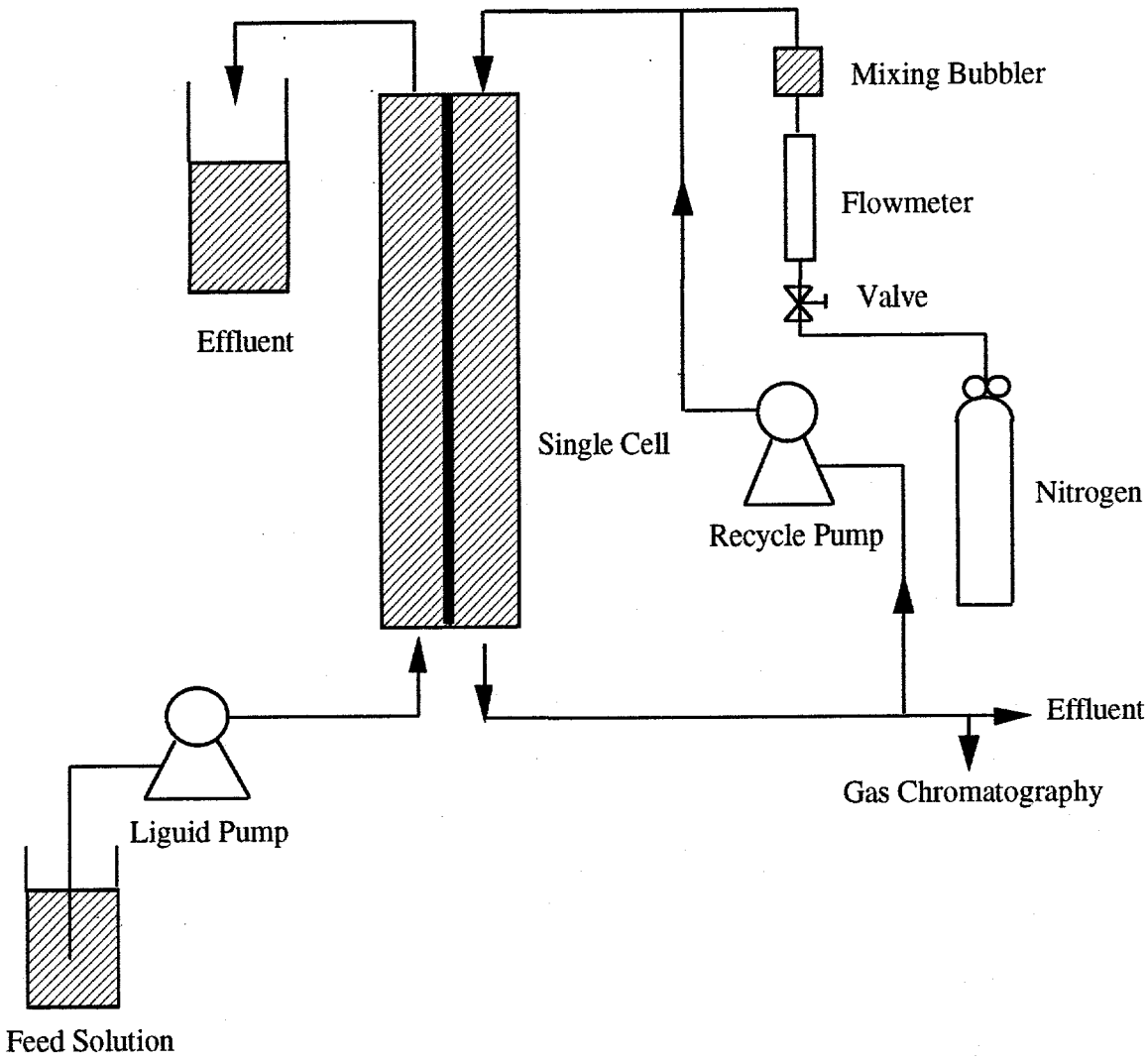

Figure 5. Schematic Diagram for Methanol Transport Apparatus.

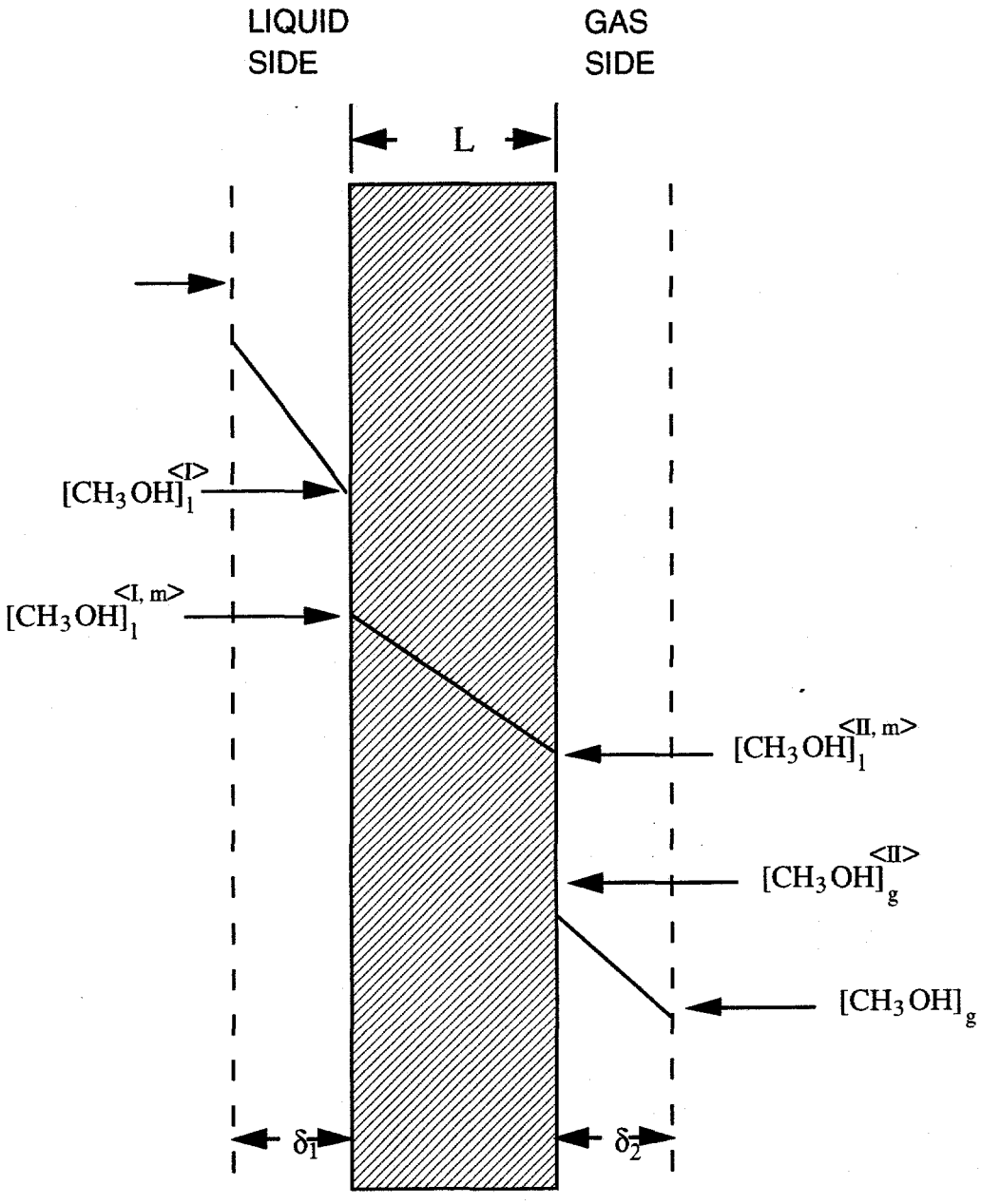

Figure 6. Schematic Diagram of Methanol Transport Mechanism Through the Membrane.

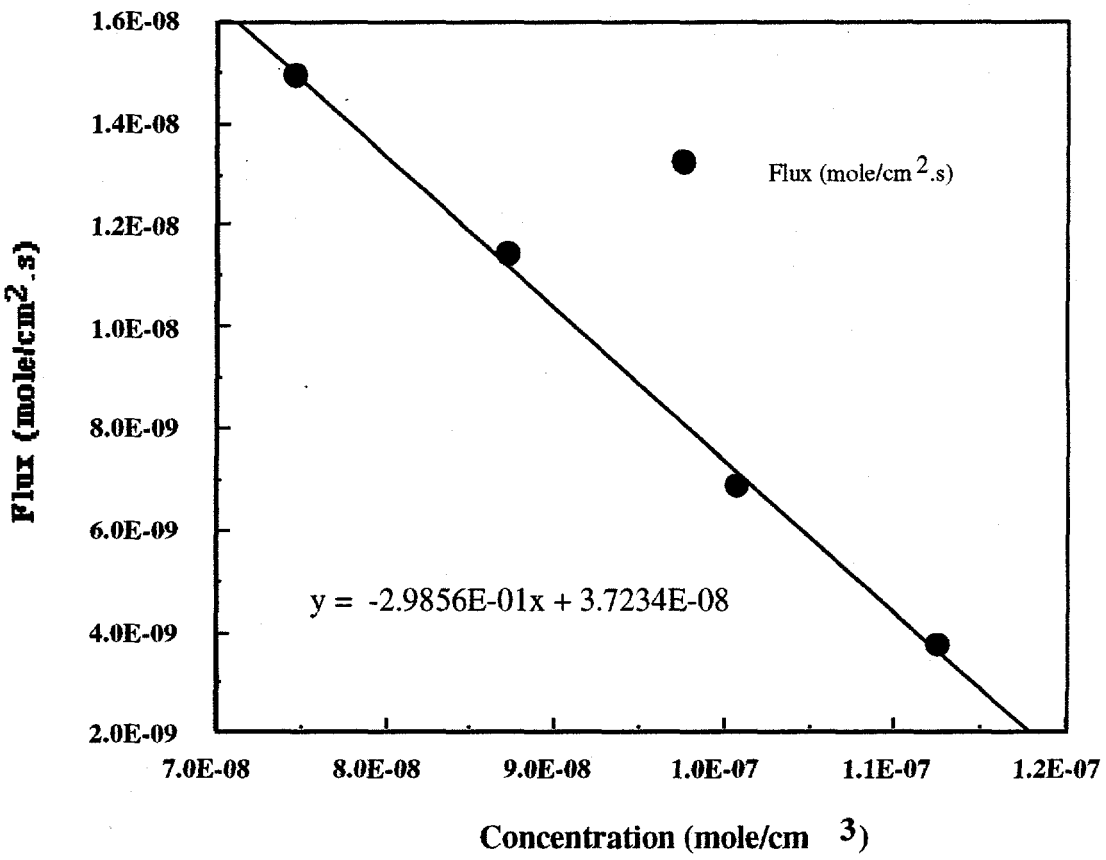

Figure 7. Plot of Methanol Flux vs Gas Phase Concentration for Commercial Nafion 117 Membrane using 0.8 M Methanol Solution at 18 °C.

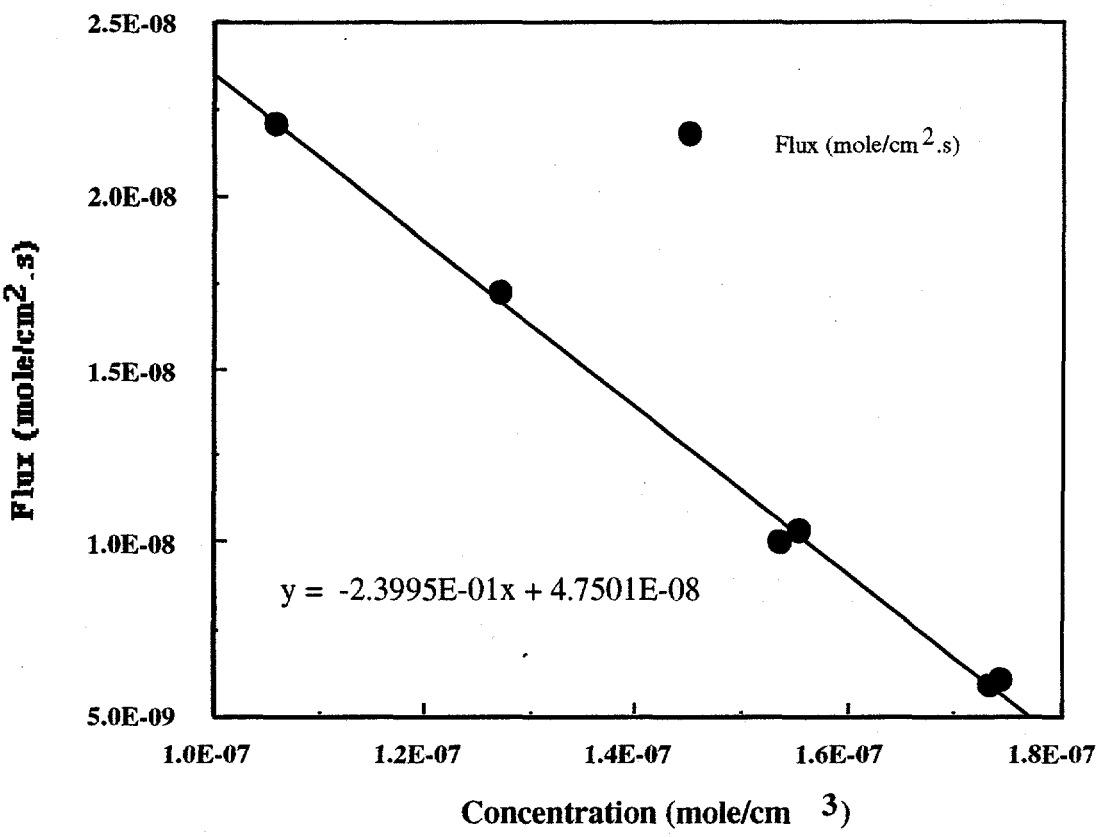

Figure 8. Plot of Methanol Flux vs Gas Phase Concentration for Commercial Nafion 117 Membrane using 1.2 M Methanol Solution at 18 °C.

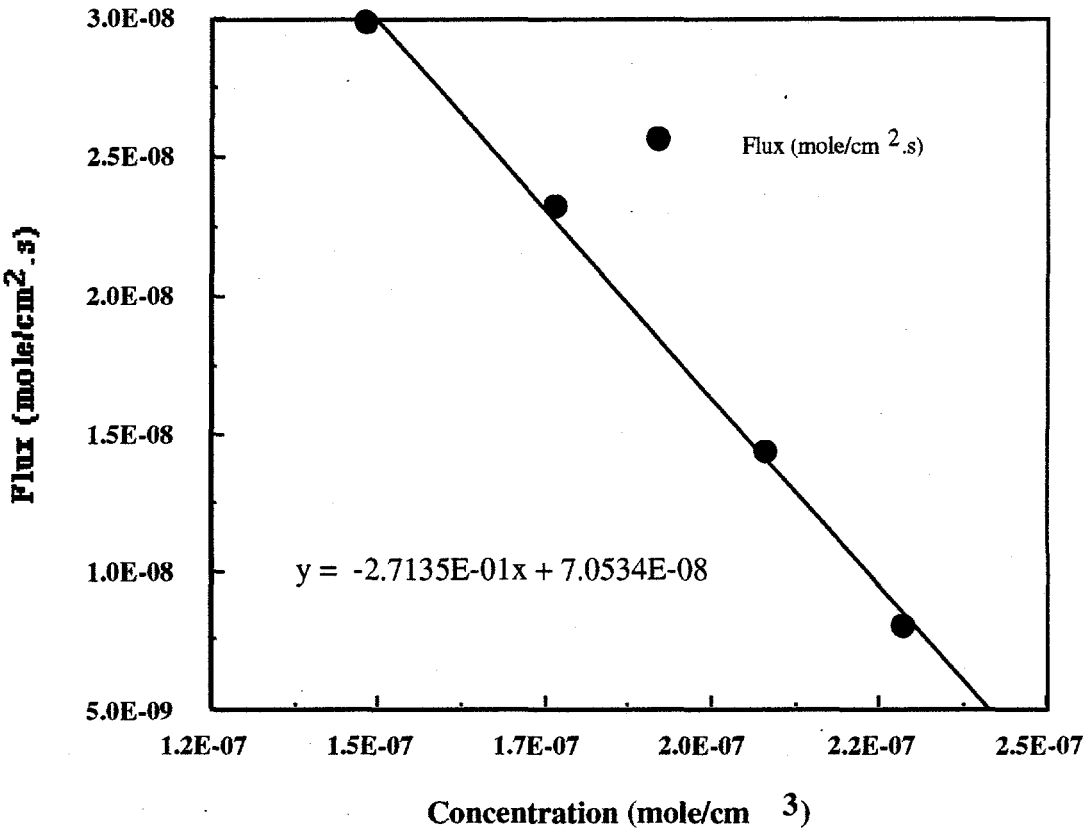

Figure 9 Plot of Methanol Flux vs Gas Phase Concentration for Commercial Nafion 117 Membrane using 1.6 M Methanol Solution at 18 °C.

C. Task 3.0: Chemically Modified Proton Exchange Membrane (J. Leddy, University of Iowa)

1. Summary

No work has yet been performed on this task.

2. Introduction

Protons can conduct through PEMs by two different mechanisms. One mechanism is physical migration of the hydrated (solvated) proton. This process carries multiple waters of hydration with each proton. The other mechanism is an exchange conduction process where a proton associates with a water molecule to form hydronium, and the proton on the other side of the ion disassociates from that ion to associate with the next water molecule.

The effect is net displacement of protons across the cell. No waters of hydration are associated with this process. Inherently, this exchange process is a more facile conduction process than physical migration of the hydrated proton. This is called the Grottius mechanism. In a hydrogen fuel cell, it is estimated that each proton that crosses the separator carries one to seven waters of hydration. This suggests that in perfluorinated separators, physical migration, while slower than Grottius conduction, is the dominant mode of transport. It can be anticipated that an analogous mechanism is possible in methanol and methanol-water mixtures.

A principal difficulty remaining with polymer separators in hydrogen/oxygen fuel cells is water management. Protons are hydrated, and as they cross the separator, they carry sufficient solvent across the cell that the anode becomes dehydrated while the cathode floods. This results in a marked decrease in cell efficiency. A similar problem can be anticipated for a methanol-oxygen fuel cell, as protons are solvated by methanol almost as well as they are hydrated by water ($CH_3OH+H_3O^+ \leftrightarrow CH_3OH_2^+ + H_2O, K_{eq}=0.23$). As materials such as Nafion$^{(R)}$ swell, about twice as much in methanol as in water, and they swell to an even greater extent in mixed solvents, the water disparity across the cell may be worse in the presence of the methanol-water fuel mixture. An additional difficulty arises because, while in a hydrogen fuel cell the water

simply floods the cathode, in a methanol fuel cell, methanol in the cathode compartment can also react with oxygen and deactivate the electrode catalyst. Fluid management is a large problem in hydrogen/oxygen fuel cells and a potentially larger problem in direct-methanol fuel cells.

3. Program

The University of Iowa will address the problem of fluid management in PEM fuel cells by tailoring composite ion exchange polymers to control solvent flow. Research will focus on composites formed with perfluorinated ion exchangers, because these materials have been tested extensively and are almost ideal for fuel cell applications, except for the fluid management problem. The composites will be designed to modify the conduction process for the proton across the membrane.

If composites can be formed that can convert the conduction mechanism in perfluorinated cation exchange polymers from predominantly physical migration to Grottius conduction, then the problem of solvent transport from anode to cathode can be addressed. Grottius type conduction can occur with primary and secondary alkyl amines.

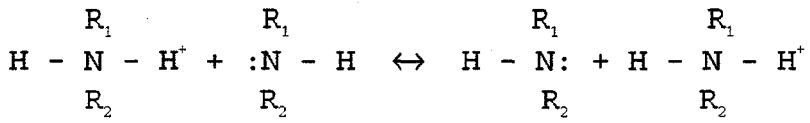

Sulfonic acids ion pair substantially with amines, so it should be possible to crosslink a sulfonic acid polymer with amines. Two things will occur. First, the crosslinking will tend to compress the polymer structure, making channels for bulk solvent transport smaller and more resistive to fluid flow. Second, if the concentration of amines is sufficiently high (roughly 1M), the amines will provide sites where protons can conduct in a Grottius exchange mechanism. If bulk solvent is sufficiently reduced, then proton conduction will be maintained by the mechanism demanding less solvent. To keep the amines from diffusing around the ion exchange matrix, polyalkyl amines (e.g. polyallylamine) will be used. Because of ion pairing between numerous sites along the polyamine chain, the transport rate of the amine will be very slow. The molecular weight of the amine can be controlled to localize the amine.

One question to be considered is whether this crosslinking of the ionomer will reduce the proton conductivity of the membrane enough to limit the fuel cell performance. It seems probable that crosslinking the ionomer will reduce its ionic conductivity. However, the performance of Nafion(R)-based hydrogen/oxygen fuel cells is not limited by membrane transport. If the conductivity is reduced substantially by crosslinking, the conductivity can be enhanced by making a microstructured composite. The University of Iowa has shown that the conductivity of Nafion(R) composite membranes can be enhanced by as much as twenty-fold by coating the Nafion(R) on an inert high surface area material, such as either polystyrene microbeads or polycarbonate neutron track etched polymers.(1,2)

The crosslinking of Nafion(R) may be particularly advantageous in the methanol fuel cells. Because of the swelling in methanol and methanol water mixtures, Nafion(R) will tend to transport more bulk solvent in the mixture than in water. Thus by crosslinking the matrix, the swelling will be reduced.

Initially, composites can be evaluated for performance using steady state rotating disk measurements for the reduction of proton to hydrogen. The rotating disk electrode will be specially modified to measure both proton flux and water transport.

4. References

(1). J. Leddy and N. E. Vanderborgh, "Microstructural Enhancement of Mass Transport Through Nafion+Nuclepore Composite Membranes", J. Electroanal. Chem., **235,** pp. 299 to 315 (1987).

(2). J. Leddy and L. Zook, "Composite Ion Exchange Materials: Flux Enhancements Through Microbead Composites", The Electrochemical Society, Extended Abstracts, **93-1**, Abstract No. 1821, pp. 2479 (1993).

III. Current Problems

A. Task 1.0: Direct Methanol Catalyst

Initial experiments with NiPC and CoPC have established the methods by which monolayers of the macrocycles can be deposited on carbon. However, coverages calculated from the charge under the peaks in cyclic voltammograms were less than calculated from the adsorption procedure. One explanation may be that the electrodes were incompletely wetted by electrolyte during voltammetry. If this proves to be the case then procedures for assuring complete utilization of the catalysts in practical electrodes will have to be developed.

Because the subcontract between UCONN and International Fuel Cells (IFC) started one month after the contract between IFC and DOE, the work being performed at UCONN is behind schedule. An additional problem resulted because the subcontract started during the summer when students already had other scheduled activities. Some of this lost time will be recovered through the use of more post-doctoral participants rather than graduate students.

B. Task 2.0: Physically Modified Proton Exchange Membrane

Composite membranes using Teflon(R) as the filler material was originally planned to be obtained from W.L. Gore & Associates, Inc. since such membranes had previously been supplied to another researcher.[1] However, these materials are not available for use in this program.

This task is also behind schedule because of the late start of the subcontract and student availability.

C. Task 3.0: Chemically Modified Proton Exchange Membrane

No work has yet been started on this task because of the late start of the subcontract with UCONN and the time necessary to obtain a person at the University of Iowa to assist in this task. Because of this lost time, a post-doctoral employee is being recruited and

---

[1] E.J. Taylor, C. Pazienza, R. Waterhouse, and G. Wilemski, "The Effect of Support Morphology on Composite Membrane Performance", The Electrochemical Society, Proceedings Vol. 86-2, Abstract No. 590, pp. 883 (1986).

should become available early in the next quarter. The use of a post-doctoral employee rather than a graduate student should help to accelerate this task.

IV. Work Planned

Task 1.0: Direct Methanol Catalyst

During the next quarter voltammograms will identify the electrochemical redox behavior of the various macrocycles. They will be screened for their activity for the catalysis of methanol oxidation, with and without platinum co-catalyst.

The relationship between the redox behavior and catalyst activity will be examined to identify a catalyst system for optimization.

Metal complexes of tetramethyl-tetraazacyclotetradecane will be synthesized at the University of Connecticut and will be included in the catalyst screening program as they become available.

Task 2.0: Physically Modified Proton Exchange Membrane

During the next quarter Nafion solution will be impregnated into polyvinylidene fluoride (PVF) membranes with various pore sizes in order to investigate the effect of pore sizes on the methanol transport. Fine powders such as silicon carbide and aluminum oxide as well as Teflon colloids will be mixed with Nafion solutions and then will be cast as composite membranes. Composite membranes will be characterized by various techniques and tested for the methanol transport. Ionic conductivity of the various membranes will be determine using AC impedance spectroscopy.

Task 3: Chemically Modified Proton Exchange Membrane

Synthesis of Nafion membranes that have crosslinking will begin. These membranes will be characterized with respect to conductivity, water transport, and methanol transport.

V. Schedule Status

The two major milestones of the subcontract at UCONN are the delivery of a membrane sample to International Fuel Cells at the end of January 1997 and the delivery of a catalyst sample at the end of February 1997. In spite of the UCONN subcontract starting behind schedule, the delivery of preliminary samples with this time schedule is still considered feasible.